systems

MDPI

Article

Dynamic Evolution and Spatial Spillover Effects of Urban Carbon Unlocking in China

Zun Yu, Zebin Zhao * and Nan Wang

School of Economics and Management, Harbin Institute of Technology, Harbin 150001, China; 21b910042@stu.hit.edu.cn (Z.Y.); wn030214@163.com (N.W.)
* Correspondence: zhaozebin@hit.edu.cn

Highlights

Please indicate how your work links to systems science via your contributions to systems practice, theory, and/or methodology.

- This study examines urban carbon unlocking as an evolving process involving interconnected industrial, technological, institutional, and social-behavioral conditions.
- It connects changes in carbon unlocking levels with state persistence, neighborhood-dependent transitions, and local and cross-city associations, providing evidence on the temporal and spatial interdependence of urban low-carbon transitions.

What are the main findings and/or the implications of the main findings?

- Urban carbon unlocking generally improved, while significant positive spatial clustering and strong state persistence remained. The highest CUL state had a 91.69% probability of remaining unchanged.
- Economic development shows a positive short-run local association with CUL, while the digital economy exhibits a negative short-run cross-city association. Both findings remain significant across alternative nearest-neighbor matrices, highlighting the importance of considering intercity relationships alongside local transition conditions.

Abstract

Reductions in emissions do not necessarily indicate substantive relief from carbon lock-in. Using panel data for 282 Chinese cities at or above the prefecture level during 2010–2024, this study constructs an urban carbon unlocking (CUL) index across four dimensions—industry, technology, institutions, and social behavior—and examines dynamic evolution, state transitions, and spatial associations through spatial Markov and dynamic Spatial Durbin analyses. CUL levels generally increased through gradual improvement, a marked rise, and subsequent adjustment, with significant positive spatial clustering throughout the study period. State transitions were gradual, with strong persistence in both low and high CUL states and limited cross-level transitions. Cities in low and intermediate states were more likely to move upward when neighboring cities exhibited higher CUL levels. Bias-corrected QML estimates indicate substantial temporal persistence and positive spatial dependence. Secondary-industry agglomeration exhibits a negative local association in the baseline model, whereas government intervention shows a positive local association. Economic development has positive short- and long-run local associations. The digital economy exhibits a negative short-run cross-city association that remains statistically significant across alternative nearest-neighbor matrices, while its long-run association is more sensitive to model specification. These findings provide evidence on the evolution, state persistence, and spatial associations of urban CUL, informing assessments of low-carbon transitions and regional environmental governance.

Check for updates

Academic Editors: Dinko Primorac and Katerina Fotova Čiković

Received: 11 October 2026
Revised: 5 November 2026
Accepted: 11 November 2026
Published: 18 November 2026

Copyright: © 2026 by the authors. Licensee MDPI, Basel, Switzerland. This article is an open access article distributed under the terms and conditions of the Creative Commons Attribution (CC BY) license.

Keywords: carbon unlocking; dynamic evolution; state transitions; spatial spillovers; neighborhood dependence

1. Introduction

Under the constraints imposed by China's carbon peaking and carbon neutrality targets, the country's low-carbon development is shifting from localized adjustments centered on pollution control, energy-efficiency improvements, and end-of-pipe emission reductions toward a systemic transition involving industrial structures, energy systems, technological pathways, institutional arrangements, and social behavior. Once a high-carbon development model becomes embedded in long-term investment, infrastructure, technological standards, and local governance systems, however, it may become continuously self-reinforcing through increasing returns to scale, sunk costs, and vested interests, making it difficult even for low-carbon technologies with environmental and economic advantages to replace existing technologies in the short term. China's coal triangle region provides a typical example of high-carbon path dependence, where long-established resource dependence, industrial structures, and energy production systems are deeply intertwined, imposing substantial carbon lock-in constraints on the low-carbon transition. The stronger the degree of carbon lock-in, the greater the potential difficulty and transition costs associated with achieving climate targets. This form of path dependence, jointly shaped by technologies, infrastructure, institutional arrangements, and behavioral norms, is generally conceptualized as "carbon lock-in" [1]. Rather than being a purely technological problem, carbon lock-in results from the interdependence and co-evolution of technologies and infrastructure, institutional arrangements, and behavioral norms [2]. A decline in current-period carbon emissions, therefore, does not necessarily imply that the existing state of carbon lock-in has been substantively alleviated. Meaningful urban carbon unlocking (CUL) therefore entails coordinated adjustments across industrial, technological, and institutional sectors, behavioral dimensions that progressively weaken the self-reinforcing mechanisms sustaining high-carbon development. In this process, cities constitute not only the primary spatial units in which industrial, technological, and institutional adjustments take place, but also an important scale at which differences in CUL emerge. Because cities differ substantially in their development foundations, industrial structures, and transition conditions, their CUL trajectories may exhibit pronounced heterogeneity [3]. Resource-based cities and cities dominated by heavy and chemical industries may face stronger constraints from established industrial systems and employment structures, resulting in greater lock-in inertia [4,5]. By contrast, cities with stronger foundations for technological innovation and industrial upgrading are more likely to ease existing carbon lock-in constraints [6]. Accordingly, focusing solely on changes in national average carbon emissions or carbon intensity makes it difficult to identify actual differences in CUL across cities or to determine whether the low-carbon transition is occurring broadly or remains concentrated in cities and regions with stronger transition advantages.

Urban CUL depends not only on local industrial, technological, and institutional conditions but also exhibits pronounced spatial interdependence. On the one hand, cities are closely connected through industrial specialization, energy supply and demand, transportation linkages, and factor mobility, meaning that their CUL trajectories do not evolve independently of one another. Green technologies may diffuse to neighboring cities through knowledge exchange and industrial linkages, environmental policies may generate demonstration effects, and carbon-intensive production activities may relocate to nearby areas in response to differences in regulatory stringency [7,8]. On the other hand, because cities

differ in their development foundations and transition capacities, spatial linkages between neighboring cities may facilitate technological diffusion and experience sharing, but may also be accompanied by industrial relocation, factor siphoning, and resource reallocation, thereby generating spatial effects in different directions. More importantly, urban CUL may exhibit temporal persistence, while its state transitions may depend on neighborhood conditions. An understanding based solely on contemporaneous spatial patterns is therefore insufficient; temporal evolution and spatial interdependence need to be examined within an integrated analytical framework.

Although theories and analytical frameworks of carbon lock-in provide an important foundation for understanding high-carbon development patterns, empirical research on low-carbon transitions has largely focused on outcome-based indicators such as carbon emissions, carbon intensity, and carbon efficiency. In recent years, research on CUL has begun to assess, from a multidimensional perspective, the extent to which cities move beyond existing lock-in conditions and has further examined policy effects and spatial interdependence. The analytical focus has thus gradually expanded from changes in emission-reduction outcomes to the weakening and evolution of carbon lock-in states [3,6,9]. Nevertheless, compared with the identification of static levels and policy effects, the dynamic nature of urban CUL, characterized by both temporal persistence and spatial interdependence, remains insufficiently understood. Of particular importance is whether intercity differences merely represent disparities in levels at particular points in time or evolve into persistent differences in states; whether cities at different levels can transition away from their existing states; and whether the states of neighboring cities shape such transitions. At the same time, industrial linkages, technological diffusion, capital flows, and policy interactions increasingly extend across city boundaries, implying that the effects associated with CUL are not confined to individual cities and may accumulate over time while operating in different directions across space. Linking long-term evolution, state transitions, and cross-regional effects is therefore essential for developing a deeper understanding of the dynamic process of urban CUL and its spatial interdependence.

In summary, this study focuses on 282 Chinese cities at or above the prefecture level over the period 2010–2024 and constructs an urban CUL index across four dimensions: industry, technology, institutions, and social behavior. The analysis follows a progressive framework of "dynamic evolution–state transitions–spatial spillovers." First, the analysis extends from static measurement to dynamic evolution by identifying the long-term evolution of urban CUL in terms of temporal changes, distributional dynamics, and spatial patterns. Second, it moves from spatial clustering to state transitions by further examining the persistence of different CUL states, the directions of state transitions, and neighborhood dependence. Finally, it examines short- and long-run spatial associations by jointly accounting for temporal persistence and spatial dependence, distinguishing local from cross-city associations and comparing their patterns across time horizons. This establishes an analytical framework that progresses from the identification of CUL levels to state evolution and, ultimately, to dynamic spatial spillovers, as illustrated in Figure 1. Accordingly, this study addresses three main questions. First, how did urban CUL in China evolve over the study period in terms of temporal trends, distributional changes, and spatial patterns? Second, do different CUL states exhibit persistence, can cities transition between states, and do neighborhood conditions alter the state transition process? Third, how are different factors associated with urban CUL, and how do their local and cross-city associations differ between the short and long run?

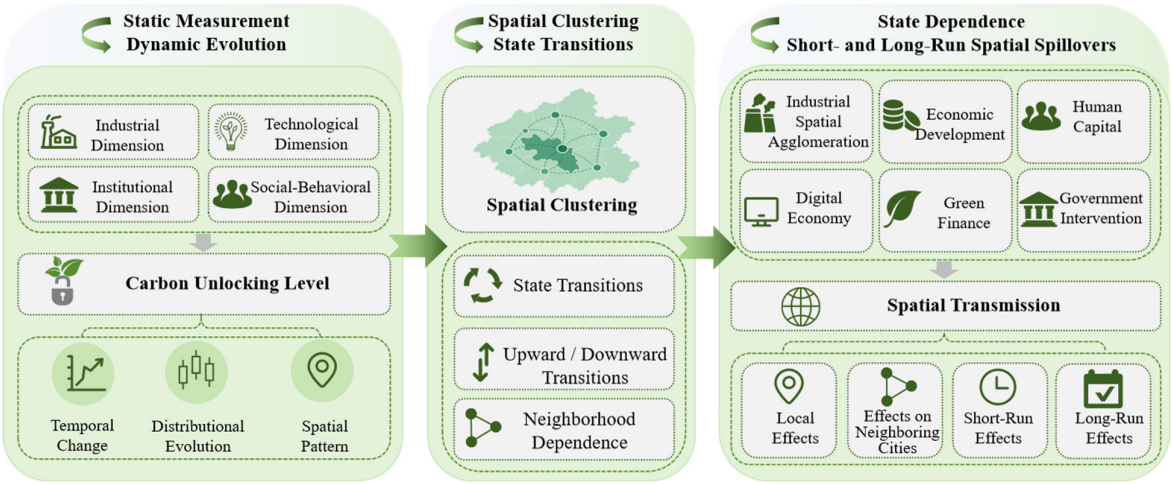


Figure 1. Research Framework.

Compared with existing studies, this study makes three contributions. First, it examines the dynamic evolution of urban CUL through long-term changes in its levels and distribution, identifying distinct stages within the overall improvement and providing empirical evidence on the progression of urban low-carbon transitions. Second, it incorporates neighborhood states into the analysis of transitions between CUL categories, revealing strong state persistence and differences in upward transition probabilities across neighborhood conditions. This provides further evidence on whether improvements in urban CUL levels are accompanied by upward movement in cities' relative positions. Third, while accounting for the temporal persistence of CUL, it distinguishes the local and spatial spillover associations of relevant factors and compares their short- and long-run patterns, providing empirical evidence on intercity linkages in urban carbon unlocking and their differences across time horizons.

The remainder of this paper is organized as follows. Section 2 reviews the literature on carbon lock-in and CUL, dynamic evolution, and spatial spillovers. Section 3 introduces the research methods, variable measurement, and data sources. Section 4 examines, in sequence, the dynamic distribution, spatial autocorrelation, state transitions, drivers, and spatial spillover effects of urban CUL. Section 5 summarizes the main findings and presents the corresponding policy implications.

2. Literature Review

2.1. Carbon Lock-In and Carbon Unlocking

Carbon lock-in originates from path dependence and technological lock-in. Technological advantages established at an early stage may become increasingly self-reinforcing through learning effects, increasing returns to scale, and network externalities, making it difficult for later-emerging alternative technologies to alter established technological trajectories in the short term even when they are more efficient [10,11]. When this logic was introduced into energy and climate research, fossil-fuel technologies were further situated within a co-evolutionary framework of technology, infrastructure, and institutions, giving rise to a self-reinforcing "carbon-based techno-institutional complex" [1]. As capital becomes increasingly embedded in existing energy and production systems, breaking away from established pathways requires coordinated adjustments not only in individual technologies but also in supporting infrastructure, investment structures, and institutional arrangements, causing transition costs to rise over time [12]. Carbon lock-in therefore does not automatically disappear with advances in renewable energy technologies.

Long-standing heating systems and infrastructure configurations may continue to generate new risks of carbon lock-in [13], while the interlocking of existing energy assets, industrial structures, and institutional interests can substantially increase the difficulty of moving away from fossil-fuel-based systems [14]. Long-term capital investment and infrastructure construction create substantial sunk costs, while new investment tends to remain concentrated around established production systems, thereby reinforcing path dependence between industrial development and energy demand [15]. Technological and infrastructural lock-in, institutional lock-in, and behavioral lock-in, therefore, tend to interact rather than operate independently [2]. Private car dependence represents a form of behavioral carbon lock-in, as car-oriented mobility can reinforce carbon-intensive travel patterns [16,17]. Evidence from global samples further suggests that the alleviation of carbon lock-in through climate assistance is reflected not only in changes in emissions but also in adjustments to energy and industrial structures, indicating that breaking away from established pathways requires simultaneous changes in resource allocation and production systems [18]. Evidence from China's urban carbon trading practices similarly shows that green technological innovation, industrial upgrading, and pro-environmental public behavior jointly constitute important channels for alleviating urban carbon lock-in [19], while resource dependence, labor structures, and institutional conditions can also generate substantial regional differences in the difficulty of low-carbon transition [20,21].

The concept of carbon unlocking (CUL) has evolved from the early notion of "escaping fossil-fuel lock-in" toward a view of low-carbon transition as two interrelated dynamic processes: the destabilization of existing high-carbon systems and the stabilization of emerging low-carbon systems [22]. Unlocking approaches can be classified into end-of-pipe, continuity, and discontinuity pathways [12], shifting the analytical focus from a general notion of "escaping lock-in" toward the relationships among different unlocking logics. CUL can also be differentiated into institutional and technological unlocking, whose relationship may take the form of complementarity, substitution, or synergy at different stages of industrial development. Institutional incentives tend to play a more important role during the early stages of industry development, whereas technological innovation gradually becomes the primary driving force as industries mature [23]. In the thermal power sector, reliance on technological progress alone, a single carbon price, or subsidies is likewise insufficient to overcome lock-in; a combination of declining technology costs, carbon markets, and policy incentives is more likely to facilitate systemic transition [24]. In the context of multiple forms of urban carbon lock-in, new energy demonstration city policies can promote CUL through the combined effects of technological progress, institutional guidance, and social transformation [25], while the joint implementation of digital and new energy policies can improve CUL efficiency through environmental attention, technological innovation, and industrial upgrading [26]. Trade openness may also facilitate access to cleaner technologies and promote green innovation, creating favorable conditions for weakening established carbon-intensive pathways [27]. These findings indicate that interactions among different institutional and technological conditions can alter the stability of established pathways. In terms of measurement, early studies primarily identified the extent of future lock-in created by existing capital stocks on the basis of infrastructure lifetimes, committed emissions, and the costs of premature retirement, thereby assessing the constraints that current investment imposes on future emission-reduction opportunities [28,29]. More recently, measurement has gradually shifted from indirectly assessing reductions in the degree of lock-in toward directly identifying CUL levels [30,31] and CUL efficiency [26,32]. Drawing on techno-institutional complex theory, Zhao et al. [33] developed an evaluation framework for urban CUL efficiency (CUE) that integrates technological and institutional inputs with economic and environmental outputs, providing an early systematic approach to the

quantitative measurement of urban CUL. Zhu and Rao [3] further constructed an urban CUL index encompassing institutional, industrial, technological, and social-behavioral dimensions, extending the measurement of CUL from efficiency evaluation to a multidimensional assessment of the extent to which path dependence is weakened. Building on this approach, Shen et al. [26] developed an urban CUL efficiency indicator within an "institution–technology–society" framework, further emphasizing the roles of different dimensions of lock-in and their coordinated changes in the CUL process. Meanwhile, Weng et al. [34] examined the degree and evolution of carbon lock-in across energy production, allocation, and use and, on this basis, identified the CUL effects of energy market-oriented reforms, suggesting that CUL can also be characterized by the extent to which existing high-carbon path dependence is weakened.

2.2. Spatiotemporal Evolution of Carbon Unlocking

CUL does not necessarily follow a steady upward trajectory but may exhibit temporal fluctuations, regional disparities, and heterogeneity across its constituent dimensions. Evidence from the Yangtze River Delta urban agglomeration shows that urban CUL generally follows a fluctuating upward trend, while the pace of evolution differs across industrial, institutional, technological, and social dimensions, accompanied by marked intercity disparities and spatial linkages [9]. In addition to direct measures of CUL, studies of carbon emission efficiency provide complementary evidence for identifying the dynamic characteristics of urban low-carbon transitions. Urban carbon emission efficiency exhibits nonlinear evolution over extended periods, with substantial differences across city types and regions, and has gradually developed spatial clustering patterns centered on urban agglomerations and major central cities [35]. Urban low-carbon development also tends to exhibit pronounced spatial clustering and cross-regional linkages. Major urban agglomerations, including Beijing–Tianjin–Hebei, the Yangtze River Delta, and the Pearl River Delta, occupy important positions in the national spatial association structure, with urban low-carbon performance increasingly shaped by cross-regional interactions [36]. The carbon emission patterns of these three urban agglomerations also exhibit hierarchical spatial structures to some extent [37]. Research on urban carbon emission efficiency in the Yangtze River Economic Belt further indicates that its spatial pattern is highly stable and characterized by pronounced path dependence and spatial lock-in. Areas with high and low efficiency do not switch randomly over short periods; rather, the persistence of similar states in neighboring areas contributes to stronger spatial integration [38]. Accordingly, identifying the spatial pattern of CUL requires further examination of both overall spatial autocorrelation and local clustering types. Research on the long-term evolution of carbon emissions in the Yangtze River Delta urban agglomeration shows that emission states in most cities are highly persistent and that transition probabilities across states are significantly associated with carbon emission levels in surrounding areas. The broader regional environment may even exert a stronger influence on state transitions than any single neighboring city, giving rise to a certain degree of club convergence [39]. Across seven urban agglomerations in the Yellow River Basin, carbon emissions likewise exhibit pronounced club convergence, spatial clustering, and siphoning effects. These spatial effects are also cumulative over time, with long-run effects exceeding short-run effects [40]. Evidence based on kernel density estimation and spatial convergence analysis further shows that the distributional evolution of urban low-carbon development is characterized by substantial regional heterogeneity and polarization, indicating that changes in mean values alone are insufficient to fully capture its dynamic distributional characteristics [41].

2.3. Driving Factors and Spatial Spillovers of Carbon Unlocking

Existing studies indicate that CUL is not driven by a single factor but is jointly shaped by multiple conditions, including industrial structure, knowledge and technological capabilities, digital development, financial support, and the institutional environment. Direct research on CUL remains relatively limited, with much of the relevant evidence derived from adjacent fields such as carbon lock-in, energy transition, green productivity, and green technological evolution [3,6]. Industrial structure and the level of economic development constitute important determinants of low-carbon transition. Specialized agglomeration may reinforce established production pathways through scale expansion and concentrated energy demand, whereas diversified agglomeration is more conducive to knowledge recombination and industrial restructuring. The environmental effects of industrial agglomeration therefore vary substantially across different forms of agglomeration [42,43]. From the perspective of technological evolution, industrial diversification can also expand the range of potential pathways through which regions enter new technological fields and reduce their dependence on established technological systems, with such effects being particularly pronounced in regions with relatively weaker development foundations [44]. Regions dependent on conventional energy sources, by contrast, often face higher transition costs, as the interdependence among energy-related employment, industrial structures, and existing production facilities may further reinforce path dependence [45,46]. The relationship between economic development and urban carbon lock-in may also be nonlinear, suggesting that the expansion of energy demand associated with economic growth and the countervailing effects of technological upgrading and structural transformation may operate simultaneously in shaping carbon lock-in [47].

The accumulation of green knowledge and digital development capabilities also shapes the extent to which regions can move beyond established high-carbon development trajectories. Regional green technological evolution depends not only on local knowledge bases; external technological linkages and knowledge connections can also broaden opportunities for regions to enter green technology fields. This is particularly important for technologically lagging regions, where technological catch-up depends more strongly on complementarities between local capabilities and external knowledge [48]. Human capital can influence the low-carbon transition by enhancing knowledge absorption, technology adoption, and innovation capacity. Existing evidence suggests that it not only constitutes an important channel through which urban carbon lock-in can be alleviated but also strengthens the energy transition effects of renewable energy policies [6,49]. Meanwhile, the interregional mobility of highly skilled labor can reshape the spatial distribution of innovation and investment, generating substantial cross-regional externalities of talent and knowledge [50]. The environmental effects of digitalization are likewise not confined to local areas. Digital development may generate cross-regional spillovers through industrial linkages, knowledge diffusion, and digital infrastructure, thereby strengthening spatial interdependence in urban low-carbon transitions [51,52]. Moreover, the development of the digital economy has been shown to significantly alleviate urban carbon lock-in [53]. Evidence from Chinese provinces reveals regional heterogeneity in the Granger predictive relationship between digital financial inclusion and carbon neutrality, with bidirectional predictive relationships observed in some provinces [54].

Financial resources also influence cities' capacity to sustain structural adjustment. Green finance can promote urban CUL, partly through its effects on green technological innovation [55]. The agglomeration of green financial activities may not only improve local carbon emission performance but also generate spatial spillovers to neighboring areas through capital formation, energy transition, and technological progress [56]. At the financial-market level, recent evidence documents time-varying connectedness among

carbon finance, green energy, artificial intelligence, and Bitcoin markets [57]. Local government fiscal allocation, public investment, and policy guidance can likewise shape the urban low-carbon transition. Evidence from urban agglomerations indicates that government intervention and its spatial variation are closely associated with changes in urban carbon emissions [58]. At the same time, inherited industrial structures, employment patterns, and institutional inequalities may interact and reinforce one another, leaving some traditional industrial regions subject to strong historical path dependence even when additional financial resources and policy support become available [59].

2.4. Research Gaps

Existing research has gradually expanded from technological lock-in to multidimensional perspectives encompassing industrial, institutional, and social-behavioral dimensions, giving rise to various quantitative approaches for identifying the degree of carbon lock-in, the level of CUL, and CUL efficiency. CUL, therefore, should not be understood simply as a reduction in emissions, but rather as a comprehensive representation of the gradual weakening of existing carbon lock-in and the broader process of low-carbon transition [2]. Overall, existing studies have laid an important foundation for understanding the multidimensional characteristics, regional disparities, and spatial interdependence of urban CUL, while leaving further scope for extension in three areas: long-term evolution, state transitions, and spatial spillovers. First, the long-term evolution of urban CUL itself warrants further investigation. Existing CUL indicators have been used primarily to identify the effects of specific policies, whereas relatively limited attention has been devoted to the long-term evolution of urban CUL levels. It is therefore necessary to examine temporal trends, distributional changes, and intercity disparities in urban CUL levels over a longer time horizon in order to develop a more comprehensive understanding of its dynamic evolution. Second, state transitions in CUL and their neighborhood dependence deserve further attention. Previous studies have extensively documented regional disparities, spatial clustering, and spatial autocorrelation in urban low-carbon development and have begun to examine the spatial patterns and regional linkages of CUL [9,35]. However, static spatial analyses mainly characterize spatial relationships among cities at particular points in time and provide relatively limited insight into whether different CUL states persist, how transitions between states occur, and whether neighborhood conditions shape these transitions. Examining CUL from the perspective of state persistence and transition can therefore provide a deeper understanding of the dynamic evolution of intercity disparities and their neighborhood dependence. Finally, the spatial effects of different drivers and their temporal differences require further distinction. Factors such as industrial agglomeration, economic development, human capital, the digital economy, green finance, and government intervention have been widely used to explain urban low-carbon transition, and their effects may also extend across city boundaries through knowledge diffusion, capital flows, industrial linkages, and policy interactions [48,56]. Existing studies have focused more heavily on contemporaneous or average spatial effects, while relatively less attention has been paid to distinguishing the local effects and spatial spillovers of different drivers and to how these effects differ between the short and long run. Accounting for temporal persistence alongside spatial dependence can therefore help distinguish local and cross-city associations and assess how their short- and long-run patterns vary across model specifications.

3. Methodology and Data

3.1. Entropy Weight Method

To comprehensively measure urban CUL, this study employs the entropy weight method to derive statistical weights based on the sample distributions of the indicators.

The method determines weights according to differences in the distributions of normalized indicator values across the sample [60]. A higher weight reflects greater statistical discriminatory power under the sample and preprocessing procedures used, rather than greater theoretical importance for carbon unlocking. By applying a consistent and reproducible weighting rule, the method reduces reliance on researchers' direct assignment of weights. First, the original indicators are normalized to eliminate differences in measurement units and magnitudes. For positive indicators, the normalization is expressed as:

$$z_{ijt} = \frac{x_{ijt} - \min\limits_{i,t}(x_{ijt})}{\max\limits_{i,t}(x_{ijt}) - \min\limits_{i,t}(x_{ijt})}$$

For negative indicators, the normalization is expressed as:

$$z_{ijt} = \frac{\max\limits_{i,t}(x_{ijt}) - x_{ijt}}{\max\limits_{i,t}(x_{ijt}) - \min\limits_{i,t}(x_{ijt})}$$

where x_{ijt} denotes the original value of indicator j for city i in year t, and z_{ijt} denotes the corresponding normalized value. After directional consistency processing, a larger indicator value represents a higher degree of CUL. Second, the proportion of indicator j corresponding to each observation is calculated as:

$$p_{ijt} = \frac{z_{ijt}}{\sum_i \sum_t z_{ijt}}$$

Based on this proportion, the information entropy of indicator j is calculated as:

$$e_j = -k \sum_i \sum_t p_{ijt} \ln p_{ijt}$$

where

$$k = \frac{1}{\ln N}$$

and N denotes the total number of city-year observations. When $p_{ijt} = 0$, $p_{ijt} \ln p_{ijt}$ defined as 0. The information utility value of indicator j is then calculated as:

$$d_j = 1 - e_j$$

and the corresponding indicator weight is determined as: $w_j = \frac{d_j}{\sum_{j=1}^{m} d_j}$, where m denotes the total number of indicators and w_j is the statistical weight assigned to indicator j. Finally, the urban CUL index is calculated using a weighted summation:

$$CUL_{it} = \sum_{j=1}^{m} w_j z_{ijt}$$

where CUL_{it} denotes the urban CUL level of city i in year t. A higher value of the index indicates a greater degree of CUL across the industrial, technological, institutional, and social-behavioral dimensions, whereas a lower value indicates stronger carbon lock-in characteristics. To reduce the influence of extreme values and skewed distributions on entropy-based weighting, all indicators are first winsorized at the 1st and 99th percentiles and then transformed using $\ln(1 + x)$. The indicators are subsequently adjusted according to their directional attributes and normalized using min–max normalization. To ensure intertemporal comparability, normalization and entropy weighting are performed using the pooled sample for the entire 2010–2024 period, and a common set of indicator weights is applied to all years.

3.2. Kernel Density Estimation

To further examine the dynamic distributional characteristics and evolutionary trends of urban CUL, this study employs kernel density estimation to characterize the distribution of CUL. Kernel density estimation is a nonparametric method that does not require prior assumptions about the form of the sample distribution. By generating continuous density curves, it can intuitively reveal the distributional location, degree of dispersion, polarization, and dynamic evolution of the variable of interest, making it suitable for analyzing temporal changes in the distribution of urban CUL. Let x denote the level of urban CUL. Its kernel density function can be expressed as:

$$f(x) = \frac{1}{Nh}\sum_{i=1}^{N} K\left(\frac{x-x_i}{h}\right)$$

where N denotes the number of sample cities, x_i denotes the CUL of city i, h is the bandwidth determined using Silverman's robust rule of thumb, and $K(\cdot)$ denotes the Gaussian kernel function. The optimal bandwidth is calculated separately for each year according to the distributional characteristics of the city sample. The Gaussian kernel function is expressed as:

$$K(u) = \frac{1}{\sqrt{2\pi}}\exp\left(-\frac{u^2}{2}\right)$$

The position, shape, and changes in the kernel density curves can reflect the distributional evolution of urban CUL. An overall rightward shift in the curve generally indicates an increase in the overall level of urban CUL. A more concentrated distribution suggests that intercity disparities may have narrowed, whereas a wider distribution and extended tails may indicate widening disparities. Bimodal or multimodal distributions may reflect a certain degree of stratification or polarization across cities. Accordingly, this study conducts kernel density estimation of CUL for selected years and compares the distributional location, peak height, number of peaks, and tail characteristics of the density curves to identify the overall evolution of urban CUL, intercity disparities, and potential stratification, thereby providing a basis for the subsequent analyses of spatial interdependence and state transitions.

3.3. Moran's I

To identify whether urban CUL exhibits significant spatial correlation, this study employs Moran's I to test the spatial clustering characteristics of CUL. Moran's I is a classical statistic for measuring spatial autocorrelation and can be used to determine whether cities with similar levels of CUL are spatially clustered, thereby providing a basis for subsequent spatial effect analysis. The global Moran's I is calculated as follows:

$$I = \frac{N}{\sum_{i=1}^{N}\sum_{j=1}^{N} w_{ij}} \cdot \frac{\sum_{i=1}^{N}\sum_{j=1}^{N} w_{ij}(x_i-\overline{x})\left(x_j-\overline{x}\right)}{\sum_{i=1}^{N}(x_i-\overline{x})^2}$$

where N denotes the number of sample cities, x_i and x_j denote the CUL values of cities i and j, respectively, $\overline{x}$ denotes the mean CUL of the sample cities, and w_{ij} represents an element of the spatial weight matrix used to characterize spatial proximity between cities. This study constructs the spatial weight matrix using the k-nearest-neighbors approach, defining the six geographically closest cities to city i as its spatial neighbors, and then row-standardizes the matrix. Moran's I generally ranges from -1 to 1. When $I > 0$ and is statistically significant, urban CUL exhibits significant positive spatial autocorrelation, indicating that cities with high CUL tend to be located near other high-CUL cities, while cities with low CUL tend to be located near other low-CUL cities. When $I < 0$ and is statistically significant, cities with different CUL levels tend to be spatially adjacent. When Moran's I is close to 0 or statistically insignificant, the spatial distribution of CUL is approximately random. On the

basis of the global spatial autocorrelation test, local Moran's I can be further used to identify local spatial clustering patterns for individual cities, expressed as:

$$I_i = \frac{x_i - \overline{x}}{m_2} \sum_{j=1}^{N} w_{ij}(x_j - \overline{x})$$

where

$$m_2 = \frac{1}{N} \sum_{i=1}^{N} (x_i - \overline{x})^2$$

According to the combination of a city's own CUL and the CUL of neighboring cities, local spatial association can be classified into four types: high-high (H-H), low-low (L-L), high-low (H-L), and low-high (L-H). H-H and L-L indicate spatial clustering of high-value and low-value cities, respectively, whereas H-L and L-H reflect local spatial heterogeneity. The statistical significance of both global and local Moran's I is assessed using 999 random permutation tests. Based on these measures, this study calculates the global Moran's I of CUL for each year and combines it with local spatial association patterns to examine the spatial dependence, clustering characteristics, and evolution of urban CUL, thereby providing a basis for subsequent analyses of spatial spillover effects and state transitions.

3.4. Spatial Markov Chain

To further characterize the dynamic transitions of urban CUL across different states and identify the influence of the spatial environment of neighboring areas on these transitions, this study employs a spatial Markov chain approach. A conventional Markov chain examines changes in a city's subsequent state primarily on the basis of its own state in the preceding period, whereas the spatial Markov chain further incorporates spatial lag conditions, thereby allowing the spatial dependence and neighborhood effects embedded in the transition process of urban CUL to be identified. First, based on fixed quartile thresholds derived from the pooled distribution of CUL over the full sample period from 2010 to 2024, urban CUL is classified into four states: State I (low level), State II (relatively low level), State III (relatively high level), and State IV (high level). The same thresholds are applied to all years to ensure intertemporal comparability of state transitions. Let S_{it} denote the state of city i in period t. The conventional Markov transition probability can then be expressed as:

$$p_{kl} = P(S_{i,t+1} = l \mid S_{it} = k) = \frac{n_{kl}}{\sum_{l=1}^{K} n_{kl}}$$

where p_{kl} denotes the probability that a city transitions from state k to state l, and n_{kl} denotes the number of city-year observations that transition from state k to state l during the study period. A $K \times K$ Markov transition probability matrix can therefore be constructed as:

$$P = \begin{bmatrix} p_{11} & p_{12} & \cdots & p_{1K} \\ p_{21} & p_{22} & \cdots & p_{2K} \\ \vdots & \vdots & \ddots & \vdots \\ p_{K1} & p_{K2} & \cdots & p_{KK} \end{bmatrix}$$

The elements on the main diagonal of the matrix represent the probability that a city remains in its original CUL state, whereas the off-diagonal elements represent the probabilities of transitions between different states. When $l > k$, the transition can be regarded as a shift to a higher CUL state; when $l < k$, it indicates a shift to a lower CUL state. On this basis, a spatial lag term is introduced to characterize the neighborhood CUL level. The spatial lag value for city i in period t is expressed as:

$$W_{it} = \sum_{j=1}^{N} w_{ij} CUL_{jt}$$

where w_{ij} is an element of the spatial weight matrix, and CUL_{jt} denotes the CUL level of neighboring city j in period t. The same fixed-quartile classification rule is then applied to the spatial lag values to identify neighborhood states, and the state transition probabilities are recalculated conditional on neighborhood state r:

$$p_{kl}^{(r)} = P\left(S_{i,t+1} = l \mid S_{it} = k,\ W_{it} = r\right)$$

where $p_{kl}^{(r)}$ denotes the conditional probability that a city in state k, with its neighborhood in state r, transitions to state l in the next period. By comparing transition probability matrices under different spatial lag conditions, it is possible to assess whether the CUL states of neighboring areas alter the state transition paths of local cities. If the transition probabilities for the same initial state differ markedly across neighborhood conditions, this indicates that state transitions in urban CUL are dependent on neighborhood conditions. If a higher-CUL neighborhood is associated with an increased probability of transitioning to a higher state, this may indicate positive neighborhood association. Conversely, if being located in a lower-CUL neighborhood is associated with a higher probability of remaining in a low state or moving to a lower state, the low-level neighborhood may exert a certain constraining effect. To test whether state transition processes differ significantly across neighborhood conditions, this study further employs a likelihood-ratio test (G^2) to compare the conditional transition probability matrices. A statistically significant test result indicates that state transitions in urban CUL exhibit significant dependence on neighborhood conditions.

3.5. Spatial Durbin Model

To further identify the spatial dependence of urban CUL and the spatial spillover effects of different drivers, this study employs spatial econometric models. In the model specification, the spatial Durbin model (SDM) is used as the core model and is compared with the spatial autoregressive model (SAR) and spatial error model (SEM). Compared with the SAR, which considers only the spatial dependence of the dependent variable, and the SEM, which primarily captures spatial correlation in the error term, the SDM incorporates spatial lags of both the dependent and explanatory variables, thereby capturing both the spatial dependence of CUL and the spatial effects associated with the explanatory variables. The baseline static SDM is specified as:

$$CUL_{it} = \rho \sum_{j=1}^{N} w_{ij} CUL_{jt} + X_{it}\beta + \sum_{j=1}^{N} w_{ij} X_{jt}\theta + \mu_i + \lambda_t + \varepsilon_{it}$$

where CUL_{it} denotes the CUL level of city i in year t; $W = (w_{ij})$ is the spatial weight matrix, for which this study adopts a row-standardized $K = 6$ nearest-neighbor matrix; ρ is the spatial autoregressive coefficient, which captures spatial dependence in CUL across neighboring cities; X_{it} denotes a set of explanatory variables affecting urban CUL; β represents the corresponding coefficients; $w_{ij}X_{jt}$ denotes the spatially lagged explanatory variables, with θ representing the corresponding coefficients; μ_i and λ_t denote city fixed effects and year fixed effects, respectively; and ε_{it} is the random disturbance term.

Given that urban CUL may exhibit pronounced temporal persistence, a static SDM alone may overlook the influence of previous CUL levels on current CUL. Therefore, a one-period temporal lag of CUL is further introduced into the static specification to construct a dynamic spatial Durbin model:

$$CUL_{it} = \tau CUL_{i,t-1} + \rho \sum_{j=1}^{N} w_{ij} CUL_{jt} + X_{it}\beta + \sum_{j=1}^{N} w_{ij} X_{jt}\theta + \mu_i + \lambda_t + \varepsilon_{it}$$

where τ is the temporal lag coefficient, capturing the persistent effect of the previous period's CUL level on current CUL, while ρ reflects the spatial dependence between the current CUL of neighboring cities and local CUL. By incorporating both temporal and

spatial lags, the dynamic SDM can simultaneously capture the temporal persistence and spatial dependence of urban CUL. We estimate the dynamic SDM using bias-corrected quasi-maximum likelihood (QML) with city and year fixed effects, following Yu et al. [61] and Lee and Yu [62]. The estimation covers 2012–2024, with CUL observations from 2011 used to construct the initial temporal lags. For the static model specifications, LM and robust LM tests are employed to identify the form of spatial dependence, the Hausman test is used to determine the fixed-effects specification, and Wald tests are conducted to assess whether the SDM can be simplified to an SAR or SEM.

Because spatial feedback mechanisms are present in the SDM, the estimated coefficients cannot be directly interpreted as the marginal effects of the explanatory variables on CUL. This study therefore further decomposes the effects into direct, indirect, and total effects. For the kth explanatory variable, the short-run impact matrix of the dynamic SDM is expressed as:

$$S_k^{SR} = (I - \rho W)^{-1}(\beta_k I + \theta_k W)$$

The average of the diagonal elements of the impact matrix represents the direct effect, reflecting the effect of a change in the explanatory variable on local CUL together with the associated spatial feedback. The average of the row sums represents the total effect, while the difference between the total and direct effects constitutes the indirect effect, capturing the spillover impact of changes in the explanatory variable on the CUL of other cities through spatial linkages. After further accounting for dynamic adjustment, and provided that the model satisfies the stability condition, the long-run impact matrix of the kth explanatory variable can be expressed as:

$$S_k^{LR} = [(1 - \tau)I - \rho W]^{-1}(\beta_k I + \theta_k W)$$

Accordingly, this study calculates the short- and long-run direct, indirect, and total effects of each explanatory variable. The short-run effects capture contemporaneous shocks and immediate spatial feedback, whereas the long-run effects further incorporate the intertemporal cumulative effects generated by the temporal persistence of CUL. Comparing short- and long-run effects makes it possible to further identify the local effects, spatial spillovers, and long-term cumulative characteristics of different drivers of urban CUL.

3.6. Variables and Descriptive Statistics

Drawing on the multidimensional approaches to identifying carbon lock-in and measuring CUL proposed by Hu and Xu [25] and Weng et al. [32], this study constructs an evaluation indicator system for urban CUL from four dimensions—industrial lock-in, technological lock-in, institutional lock-in, and social-behavioral lock-in—comprising a total of 12 indicators. Indicators that contribute to alleviating carbon lock-in are defined as positive indicators, whereas those reflecting dependence on high-carbon development are defined as negative indicators. All indicators are adjusted to ensure directional consistency before the entropy weight method is applied. The definitions and directions of the specific indicators are presented in Table 1.

Industrial lock-in is characterized by the carbon emission intensity of fixed asset investment, the share of secondary-industry value added, and dependence on foreign trade. The first two indicators reflect the high-carbon dependence of capital investment and industrial structure and are therefore defined as negative indicators. Dependence on foreign trade is treated as a positive indicator because it proxies access to external markets and opportunities for technology exchange, which can support low-carbon transitions. Fixed asset investment and GDP are measured at comparable prices, whereas total imports and exports and GDP used to calculate dependence on foreign trade are measured at current prices. Technological lock-in is characterized by the carbon intensity of energy consumption,

carbon emission intensity, and green technological innovation. The carbon intensity of energy consumption is measured as the ratio of CO_2 emissions to energy consumption converted into standard coal equivalent, while carbon emission intensity is measured as the ratio of CO_2 emissions to real GDP; both are defined as negative indicators. Green technological innovation is measured by the number of green technology patents granted and is defined as a positive indicator. Energy consumption is calculated by converting total electricity consumption, natural gas supply, and liquefied petroleum gas supply into standard coal equivalent and then aggregating them. Institutional lock-in is characterized by the share of fiscal expenditure on energy conservation and environmental protection, government attention to energy conservation and emission reduction, and the share of fiscal expenditure on science and technology. The two fiscal expenditure indicators are measured as the respective shares of general public budget expenditure, while government attention to energy conservation and emission reduction is measured by the frequency of relevant keywords in annual municipal government work reports. All three indicators are defined as positive indicators. Social-behavioral lock-in is characterized by private car ownership, public environmental attention, and the gas penetration rate. Private car ownership is treated as a negative indicator because it proxies urban reliance on private motorized travel, a potential source of social-behavioral carbon lock-in. Public environmental attention is measured using the annual Baidu Search Index for the keyword "environmental pollution" and is coded positively to reflect the potential role of public attention in environmental oversight. Public attention may also rise as pollution worsens [63]. The gas penetration rate is coded positively because access to gas can support a shift away from household coal use where gas replaces coal, as documented for residential heating in Linfen [64]. The indicator measures access to gas services, and its implications for carbon emissions depend on actual fuel substitution.

The research data are mainly drawn from the China City Statistical Yearbook, China Urban Construction Statistical Yearbook, provincial and municipal statistical yearbooks and statistical bulletins, local government work reports, EDGAR, CNRDS, and the Baidu Index. Considering consistency in indicator definitions, continuity of the city sample, and data availability, the final sample comprises 282 cities at or above the prefecture level over the period 2010–2024, forming a balanced panel of 4230 city-year observations. Descriptive statistics for the 12 underlying indicators of CUL are reported in Table 2. To ensure intertemporal comparability, monetary variables related to economic scale are adjusted for price changes. Specifically, city GDP is deflated to constant 2010 prices using provincial GDP indices, while fixed asset investment is converted to constant 2010 prices using the fixed asset investment price index. For dependence on foreign trade, both total imports and exports and GDP are measured at current prices to ensure consistency in the price basis of the numerator and denominator. Missing values are first manually verified and supplemented using local statistical yearbooks, statistical bulletins, and publicly available government information. Observations that remain unavailable are imputed using predictive mean matching within the multiple imputation by chained equations framework (MICE-PMM). The imputation model includes linear and quadratic year terms and city fixed effects. A total of 30 imputed datasets are generated, with five nearest-neighbor donor candidates and eight iterations per imputed dataset, and the median of the 30 imputed values for each missing observation is used as the final imputed value. Across the 12 CUL indicators during 2010–2024, 2547 of 50,760 observations (5.02%) were missing and imputed. Across the seven regression covariates during 2012–2024, 1149 of 25,662 observations (4.48%) were missing and filled. Sensitivity analyses excluding cities and indicators with high missingness are reported in Section 4.6.

Table 1. Indicator system for measuring urban carbon unlocking.

Primary Dimension	Secondary Indicator	Definition	Unit	Direction
Industry	Carbon emission intensity of fixed asset investment	CO_2 emissions/fixed asset investment	10,000 tons/RMB million	−
	Share of secondary-industry value added	Secondary-industry value added/GDP × 100%	%	−
	Dependence on foreign trade	Total imports and exports/GDP × 100%	%	+
Technology	Carbon intensity of energy consumption	CO_2 emissions/energy consumption converted into standard coal equivalent	10,000 tons/10,000 tons of standard coal	−
	Carbon emission intensity	Urban carbon emissions/GDP	tons/RMB 10,000	−
	Number of granted green technology patents	Total number of green technology patents granted	patents	+
Institution	Share of fiscal expenditure on energy conservation and environmental protection	Fiscal expenditure on energy conservation and environmental protection/general public budget expenditure × 100%	%	+
	Government attention to energy conservation and emission reduction	Frequency of keywords related to energy conservation, emission reduction, low-carbon development, and green development in government work reports	count	+
	Share of science and technology expenditure	Science and technology expenditure/general public budget expenditure × 100%	%	+
Social behavior	Private car ownership	Number of privately owned vehicles	1000 vehicles	−
	Public environmental attention	Annual Baidu Search Index for the keyword "environmental pollution"	index	+
	Gas penetration rate	Urban gas penetration rate	%	+

Note: "+" indicates that a higher value contributes to a higher level of carbon unlocking, whereas "−" indicates that a higher value reflects stronger carbon lock-in.

Table 2. Descriptive Statistics of Indicators Used to Measure CUL.

Variable	Mean	Std. Dev.	Min	Max
Carbon emission intensity of fixed asset investment	5.1681	9.5803	0.0260	100.8058
Share of secondary-industry value added	44.6206	11.2436	9.5700	89.7500
Dependence on foreign trade	0.1804	0.2871	0.0000	2.7121
Carbon intensity of energy consumption	27.5877	41.6007	0.4396	640.1639
Carbon emission intensity	2.0352	1.7582	0.0903	16.1266
Number of granted green technology patents	488.6331	1401.6338	0.0000	20,687.0000
Share of fiscal expenditure on energy conservation and environmental protection	0.0295	0.0178	0.0014	0.4583
Government attention to energy conservation and emission reduction	172.5713	53.3380	0.0000	549.0000
Share of science and technology expenditure	0.0176	0.0176	0.0005	0.1743
Private car ownership	651.0224	768.1518	15.4000	8553.8890
Public environmental attention	20.4481	23.2167	0.0000	140.3644
Gas penetration rate	94.2127	11.0958	10.9900	100.0000

Note: All variables have 4230 observations.

4. Empirical Results

4.1. Measurement Results of Urban Carbon Unlocking

Based on the entropy weight method, this study calculates the urban CUL index for Chinese cities from 2010 to 2024, with its annual distributional characteristics shown in Figure 2. Overall, urban CUL levels in China generally increased over the study period, with steady improvement followed by a marked rise and subsequent adjustment at relatively high levels. From 2010 to 2016, the overall changes were relatively moderate. After 2017, both the median and mean increased markedly, reaching relatively high levels during 2019–2021. Although CUL levels declined slightly after 2022, they remained substantially higher than at the beginning of the study period. Meanwhile, the interquartile range did not narrow noticeably as the overall level increased, indicating that intercity disparities did not exhibit significant convergence. The annual mean generally remained above the median, accompanied by persistent high-value outliers, suggesting a moderately right-skewed distribution of CUL, with some cities consistently recording relatively high CUL levels. Overall, urban CUL in China improved substantially during the study period, although disparities across cities remained evident.

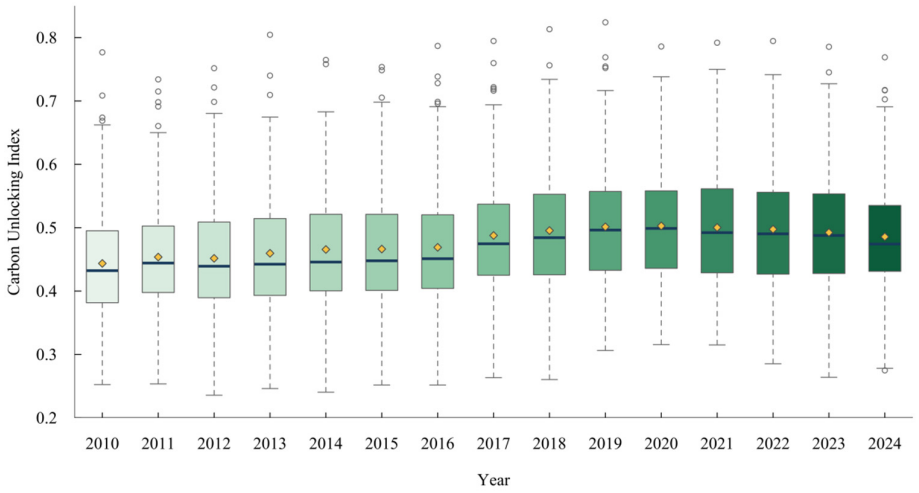


Figure 2. Boxplot Distribution of the Urban Carbon Unlocking Index in China, 2010–2024.

To examine sensitivity to the aggregation method, we recalculated urban CUL using entropy-weighted TOPSIS while retaining the baseline normalized indicators and entropy weights. The Pearson and Spearman correlations between the two indices are 0.9797 and 0.9791, respectively, indicating close agreement under the two aggregation methods. Sensitivity to alternative weighting schemes is examined in Section 4.6.

From a spatial perspective, Figure 3 presents the spatial distribution of CUL across Chinese cities in 2010, 2015, 2020, and 2024. To ensure comparability across different points in time, the city samples from the four years are pooled and classified into five categories using the Jenks natural breaks method, with the same classification thresholds applied to each year. In the figure, colors from light to dark represent CUL levels from low to high, while white areas indicate regions with no data. In 2010, cities with relatively high CUL were mainly distributed along the eastern coast, in parts of Northeast China, and in a small number of central and western cities, forming a relatively dispersed spatial pattern, while most cities in central China and some inland areas remained at low or medium-low levels. After 2015, the number of cities at medium-high and high levels gradually increased, with stronger high-value concentrations emerging along the southeastern coast, in the middle and lower reaches of the Yangtze River, and in parts of Northeast China. Some

neighboring cities also began to form relatively continuous high-value clusters. By 2020, the coverage of medium-high and high-level cities had expanded further, particularly in the eastern coastal and central regions. This pattern was consistent with the increases in both the annual mean and minimum CUL values, indicating that improvements had extended beyond a small group of high-performing cities to a broader range of cities. In 2024, cities with relatively high CUL remained concentrated mainly in the eastern coastal, central, and parts of northeastern regions, while the intermingling of cities across different CUL levels became more pronounced and some areas experienced shifts in classification, suggesting that although urban CUL continued to improve overall, regional differentiation also became increasingly evident.

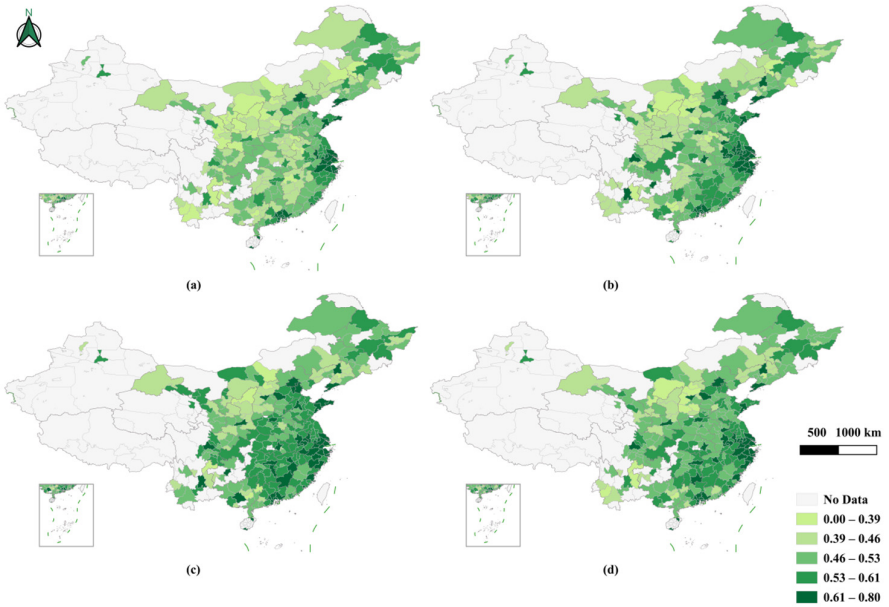


Figure 3. Spatial Distribution of Urban Carbon Unlocking Levels in China in 2010, 2015, 2020, and 2024. Note: Panels (**a**–**d**) represent 2010, 2015, 2020, and 2024, respectively. This figure was produced using a standard map downloaded from the Standard Map Service of the Ministry of Natural Resources, with map approval number GS(2024)0650. No modifications were made to the base-map boundaries.

Overall, from 2010 to 2024, urban CUL in China exhibited an evolutionary pattern characterized by simultaneous overall improvement and regional differentiation. On the one hand, the annual mean increased overall, and low-level cities also showed marked improvement during certain periods, indicating that the process of urban CUL was supported by relatively broad-based progress. On the other hand, high-level cities maintained their relative advantages over the long term and remained spatially concentrated mainly along the eastern coast, in central China, and in parts of Northeast China, suggesting that differences in CUL levels persisted across cities. Overall, the spatial pattern of urban CUL in China gradually evolved from an early configuration of localized high-value areas toward one characterized by broader improvement alongside persistent regional disparities.

4.2. Dynamic Distribution of Urban Carbon Unlocking

To characterize the temporal evolution of the distribution of urban CUL levels, kernel density estimation is conducted for 2010, 2015, 2020, and 2024, with the results presented in Figure 4. Figure 4a shows that the distribution of urban CUL levels exhibits distinct temporal changes over the study period. The main peaks of urban CUL levels in 2010 and 2015 are located at approximately 0.419 and 0.430, respectively, indicating that CUL levels were generally low in the early years of the study period and improved only moderately. In

2020, the density curve shifted markedly to the right, with the modal CUL level reaching 0.504 and the mean reaching 0.503, indicating a relatively broad-based improvement in urban CUL levels. In 2024, the modal CUL level shifted back to 0.458, and the mean fell to 0.486, indicating a partial decline in CUL levels relative to 2020, although the overall level remained higher than in 2010 and 2015. In terms of distributional shape, the relatively flat curve in 2020 suggests greater intercity dispersion, whereas the higher peak and narrower distribution in 2024 indicate increased concentration in the distribution of urban CUL levels.

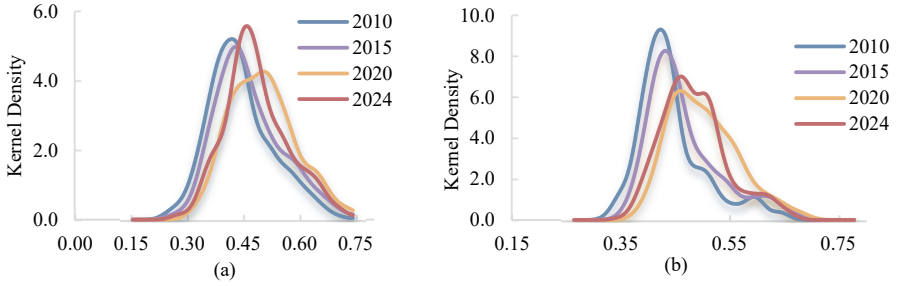


Figure 4. Kernel Density Distributions of Urban Carbon Unlocking Levels and Spatial Lags in 2010, 2015, 2020, and 2024. Note: Panel (**a**) shows urban carbon unlocking levels, and panel (**b**) shows their spatial lag values.

As shown in Figure 4b, the kernel density curves of the spatial lag values ge nerally follow a temporal trajectory similar to that of cities' own CUL levels. The main peaks are located at approximately 0.424 and 0.432 in 2010 and 2015, respectively, and at approximately 0.460 and 0.461 in 2020 and 2024, indicating an overall improvement in CUL levels in neighboring areas. The standard deviation of the spatial lag values ranges from 0.061 to 0.067, notably lower than the 0.086–0.091 range for cities' own CUL levels, indicating a more concentrated distribution of neighborhood CUL levels. In 2020 and 2024, the curves exhibit modest shoulder peaks in the medium-to-high range, but no persistent and clearly defined bimodal pattern emerges, suggesting some local heterogeneity in the distribution of spatial lag values in certain years. Overall, cities' own CUL levels and neighborhood CUL levels exhibit broadly consistent evolutionary patterns, providing preliminary evidence for the subsequent analyses of spatial autocorrelation and state transitions.

4.3. Spatial Autocorrelation of Urban Carbon Unlocking

As reported in Table 3, global Moran's I is significantly positive in every year of the sample period, ranging from 0.421 to 0.510, with $p = 0.001$ for each two-sided permutation test. This indicates that urban CUL levels in China are not randomly distributed across space but exhibit significant and persistent positive spatial autocorrelation. In other words, cities with similar CUL levels tend to be geographically clustered, with pronounced H-H and L-L clustering. From a temporal perspective, global Moran's I increased from 0.463 in 2010 to 0.487 in 2011 and, despite modest fluctuations thereafter, generally remained at a relatively high level, reaching a sample-period peak of 0.510 in 2017, indicating a strengthening of spatial clustering in urban CUL levels during this period. After 2018, global Moran's I showed an overall downward trend, declining from 0.486 in 2018 to 0.421 in 2024, suggesting that the overall degree of spatial autocorrelation in urban CUL weakened, although positive spatial autocorrelation remained statistically significant.

Local Moran's I and LISA classifications further reveal the specific types of spatial clustering (Figures 5 and 6). Overall, statistically significant clusters are dominated by H-H and L-L patterns, whereas H-L and L-H spatial outliers are relatively rare. The number of H-H cities increased from 32 in 2010 to 39 in 2017, fluctuated thereafter, and stood at 34 in 2024. Shanghai, Guangzhou, Shenzhen, Hangzhou, Ningbo, Wuxi, Changzhou, Nantong,

Jiaxing, Dongguan, and Foshan consistently exhibited H-H clustering in multiple years, indicating relatively stable clusters of high CUL levels in regions such as the Yangtze River Delta and Pearl River Delta. The number of L-L cities increased from 17 in 2010 to 33 in 2024, showing an overall upward trend. Baotou, Qingyang, Yan'an, Linfen, Shizuishan, Yulin, and Lüliang frequently exhibited L-L clustering, indicating persistent spatial clustering among some cities with low CUL levels. Meanwhile, the numbers of H-L and L-H cities remained small throughout the sample period, suggesting that the spatial pattern of urban CUL was dominated by clustering among cities with similar CUL levels rather than by spatial outliers.

Table 3. Global Spatial Autocorrelation Test Results for Urban Carbon Unlocking Levels, 2010–2024.

Year	Moran's I Index	Z Score	*p* Value	Year	Moran's I Index	Z Score	*p* Value
2010	0.4632	14.651	0.001	2018	0.4865	14.976	0.001
2011	0.4867	15.568	0.001	2019	0.4491	14.077	0.001
2012	0.4845	15.495	0.001	2020	0.4395	13.408	0.001
2013	0.4801	14.973	0.001	2021	0.4372	13.561	0.001
2014	0.4552	14.134	0.001	2022	0.4420	13.760	0.001
2015	0.4854	14.930	0.001	2023	0.4301	13.698	0.001
2016	0.4970	15.300	0.001	2024	0.4214	12.990	0.001
2017	0.5105	16.696	0.001				

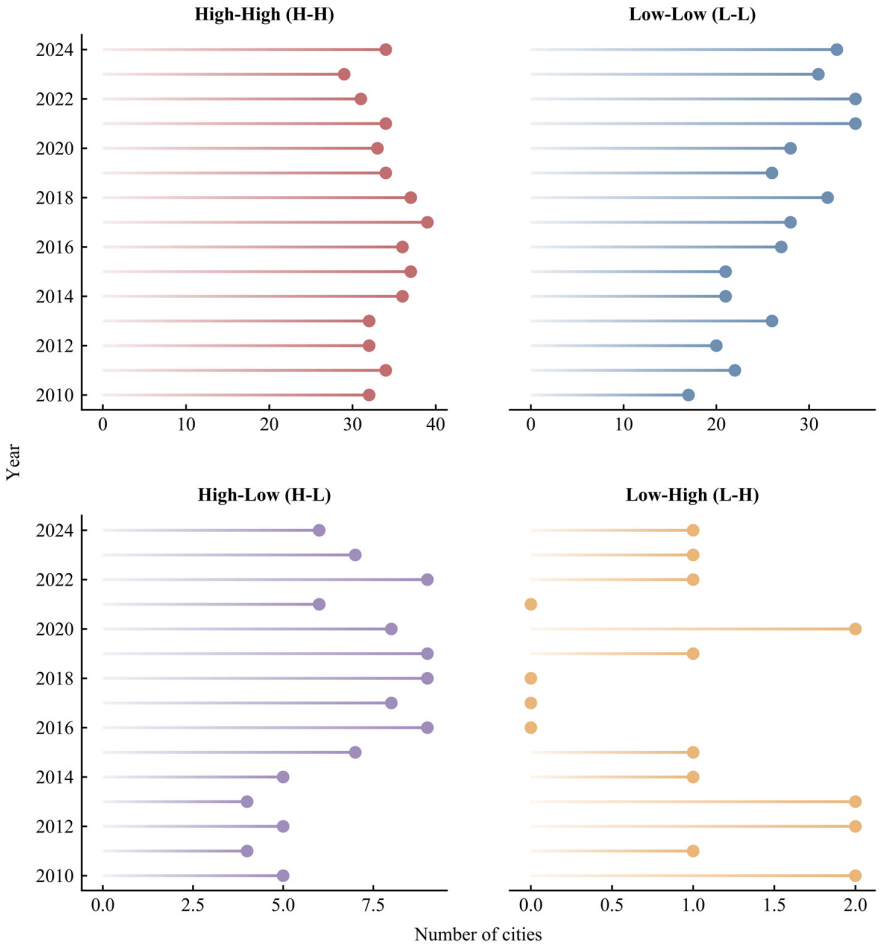


Figure 5. Changes in the Number of Local Spatial Association Types of Urban CUL, 2010–2024.

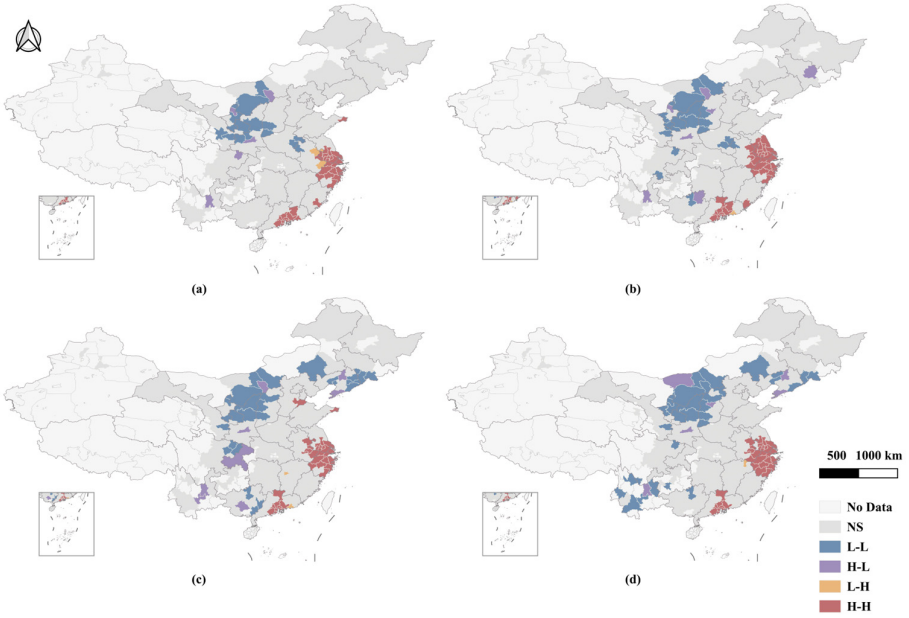


Figure 6. Local Spatial Autocorrelation Patterns of Urban Carbon Unlocking Levels in 2010, 2015, 2020, and 2024.Note: Panels (**a**–**d**) represent 2010, 2015, 2020, and 2024, respectively.

Overall, urban CUL in China exhibits persistently significant positive spatial autocorrelation, with H-H and L-L clustering as the dominant patterns. Although the overall degree of spatial autocorrelation has declined in recent years, some high-value and low-value clusters remain highly persistent, indicating a certain degree of stability in the spatial pattern of urban CUL. Building on these findings, the next section further examines the persistence, transition patterns, and neighborhood dependence of different CUL states.

4.4. State Transitions of Urban Carbon Unlocking

To further examine the state evolution of CUL and its neighborhood dependence, this study first constructs a conventional Markov transition probability matrix and then incorporates spatial lag states to estimate spatial Markov transition probabilities under different neighborhood conditions. A Sankey diagram is also used to visualize the main state transition paths. The conventional Markov transition probability matrix of urban CUL states reported in Table 4 shows that transition probabilities are concentrated primarily along the main diagonal. Based on the fixed quartile thresholds derived from the pooled sample, the probabilities of remaining in State I (low level), State II (relatively low level), State III (relatively high level), and State IV (high level) are 81.62%, 67.04%, 73.95%, and 91.69%, respectively, indicating strong state persistence and path dependence in CUL. State IV exhibits the highest persistence probability, with only an 8.31% probability of shifting downward to State III in the subsequent period, suggesting that once cities enter State IV, they tend to remain in that state. The persistence probability of State I also exceeds 80%, indicating pronounced low-state persistence among cities with low CUL levels. Overall, transitions across CUL states exhibit strong persistence.

In terms of transition distance, changes in CUL states occur predominantly between adjacent states, whereas transitions across multiple states are highly limited (Figure 7). The probability of moving from State I to State II is 17.98%, while the probability of moving directly to State III is only 0.40%, and no direct transition to State IV is observed. The probability of moving from State II to State III is 20.84%, whereas the probability of moving directly to State IV is only 0.10%. Downward transitions from State IV are likewise confined to State III. These results indicate pronounced gradualism in CUL state transitions, with

most movements occurring between adjacent states and transitions across non-adjacent states remaining relatively rare. Thus, even when cities in lower states improve, they are more likely to move first into an adjacent state rather than directly into a high state. By comparison, the intermediate states exhibit greater mobility. State II has the lowest persistence probability, at 67.04%, and its probability of moving upward to State III (20.84%) exceeds its probability of falling back to State I (12.01%), indicating that cities in State II are more likely to move to State III than to State I. For State III, the probability of moving upward to State IV is 11.08%, while the combined probability of falling to lower states is 14.98%. This suggests that although cities in State III have established a foundation for further improvement, whether they can advance to State IV remains uncertain. State III therefore exhibits divergent transition patterns: some cities advance to State IV, whereas others move to lower CUL states.

Table 4. Conventional Markov Transition Probability Matrix of Urban CUL States.

t \ $t+1$	Sample Size	State I	State II	State III	State IV
State I	1012	81.62%	17.98%	0.40%	0.00%
State II	974	12.01%	67.04%	20.84%	0.10%
State II	975	0.31%	14.67%	73.95%	11.08%
State IV	987	0.00%	0.00%	8.31%	91.69%

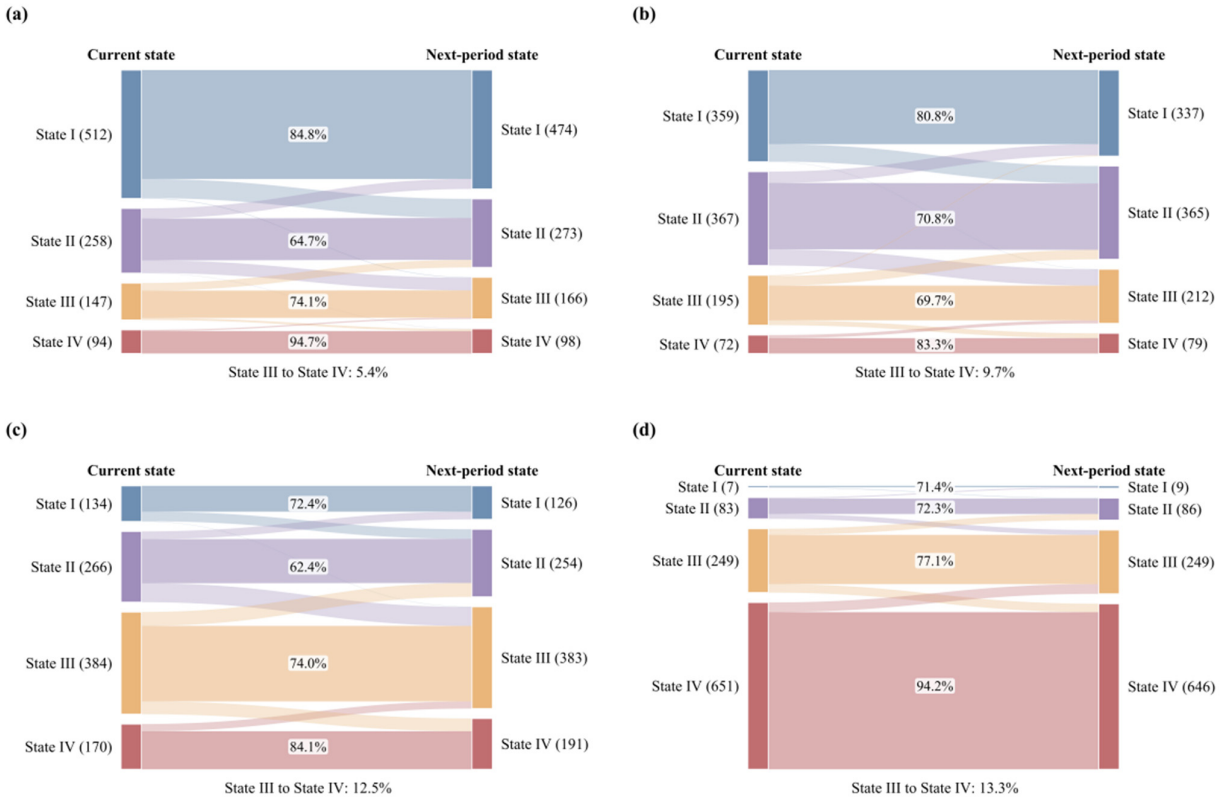


Figure 7. Sankey Diagrams of Urban Carbon Unlocking State Transitions under Different Neighborhood Conditions. Note: Panels (**a**–**d**) show neighborhood States I–IV. Line width indicates transition frequency; node counts and flow percentages indicate observations and state persistence, respectively. State III-to-IV transition probabilities appear below each panel.

After spatial neighborhood conditions are taken into account, state transitions exhibit clear spatial heterogeneity (Table 5). The overall likelihood-ratio statistic for the test of spatial conditional independence is $G^2 = 81.164$ with 27 degrees of freedom and $p < 0.001$,

rejecting the null hypothesis that state transitions are independent of neighborhood states and indicating significant neighborhood-condition dependence in CUL state transitions. State-specific tests show that differences across neighborhood conditions are significant at the 5% level for State II, State III, and State IV, with State III and State IV significant at the 1% level, while State I is significant at the 10% level. This indicates that neighborhood conditions are associated with state transitions differently across initial states, with stronger statistical evidence among cities in intermediate and high states. Table 5 and Figure 7 further reveal the direction of these neighborhood associations. For cities in State I, the probability of remaining in the same state declines as the neighborhood state rises from State I to State III, from 84.77% under a State I neighborhood to 80.78% and 72.39% under State II and State III neighborhoods, respectively; correspondingly, the probability of an upward transition rises from 15.23% to 19.22% and 27.61%. A clearer spatial gradient appears in transitions from State III to State IV. As the neighborhood state rises from State I to State IV, the transition probability increases successively from 5.44% to 9.74%, 12.50%, and 13.25%, suggesting that the association with higher-state neighborhoods is more pronounced for cities that have already established a certain foundation for CUL. Thus, higher-state neighborhoods are associated with a greater probability of transition to a higher state, although the strength of this neighborhood association varies with the city's initial state. Cities in State IV exhibit strong state persistence, with persistence probabilities exceeding 83% under all neighborhood conditions and reaching 94.68% and 94.16% under State I and State IV neighborhoods, respectively. This indicates that State IV itself is highly persistent, while its persistence probability does not increase monotonically with the neighborhood state. Overall, neighborhood conditions are associated with heterogeneous transition patterns across initial states: cities in low and intermediate states are more sensitive to changes in neighborhood states, whereas State IV exhibits strong persistence.

Table 5. Spatial Markov Transition Probabilities of Urban Carbon Unlocking States under Different Neighborhood Conditions.

Neighborhood State	Current State (t)	Sample Size	Next Period State (t + 1)			
			State I	State II	State III	State IV
State I	State I	512	84.77%	14.84%	0.39%	0.00%
	State II	258	15.50%	64.73%	19.38%	0.39%
	State II	147	0.00%	20.41%	74.15%	5.44%
	State IV	94	0.00%	0.00%	5.32%	94.68%
State II	State I	359	80.78%	18.94%	0.28%	0.00%
	State II	367	11.99%	70.84%	17.17%	0.00%
	State II	195	1.54%	18.97%	69.74%	9.74%
	State IV	72	0.00%	0.00%	16.67%	83.33%
State III	State I	134	72.39%	26.87%	0.75%	0.00%
	State II	266	10.90%	62.41%	26.69%	0.00%
	State III	384	0.00%	13.54%	73.96%	12.50%
	State IV	170	0.00%	0.00%	15.88%	84.12%
State IV	State I	7	71.43%	28.57%	0.00%	0.00%
	State II	83	4.82%	72.29%	22.89%	0.00%
	State III	249	0.00%	9.64%	77.11%	13.25%
	State IV	651	0.00%	0.00%	5.84%	94.16%

4.5. Driving Factors and Spatial Spillover Effects of Urban Carbon Unlocking

The analysis considers industrial agglomeration, economic development, human capital, the digital economy, green finance, and government intervention as factors associated with CUL. The digital economy and green finance indices follow Cheng et al. [51] and

Liu et al. [55], respectively; data for the remaining covariates are mainly obtained from the China City Statistical Yearbook. CUL is the dependent variable, with its one-period lag included to capture temporal persistence. Variable definitions, units, and descriptive statistics are reported in Table 6.

Table 6. Descriptive Statistics for Variables Used in Spatial Panel Models.

Variable	Variable Definition	Unit	Mean	Std. Dev.	Min	Max
CUL	Composite CUL index	Composite index	0.4827	0.0928	0.2356	0.8241
L.CUL	One-period lag of the composite CUL index	Composite index	0.4803	0.0930	0.2356	0.8241
SIA	Secondary-industry agglomeration level	Location quotient	1.0178	0.2362	0.2593	1.9076
TIA	Tertiary-industry agglomeration level	Location quotient	0.8890	0.1765	0.2773	1.8488
lnPGDP	Natural logarithm of real GDP per capita	Logarithmic value	10.7580	0.5392	8.9292	12.4401
HC	Density of students enrolled in regular higher education institutions	Students per 100 people	1.9363	2.0018	0.0000	18.5880
DIG	City-level digital economy development	Composite index	0.0402	0.0537	0.0016	0.8608
GF	City-level green finance development	Composite index	0.1877	0.0856	0.0200	0.7949
GOV	Degree of government intervention	Local fiscal expenditure/GDP	0.2041	0.1008	0.0560	0.8717

Note: The estimation sample covers 282 cities from 2012 to 2024, yielding 3666 city-year observations. The dynamic QML model uses the 2011 CUL values as initial observations.

Table 7 reports specification tests for the static spatial panel models. As shown in Table 7, both the LM and robust LM tests are significant at the 1% level, indicating the presence of both spatial lag dependence and spatial error dependence. The Hausman test supports the fixed-effects specification, while the Wald tests further reject the null hypotheses that the SDM can be simplified to either the SAR or the SEM. These results support the use of a static SDM with city and year fixed effects. To account for temporal persistence in CUL, we then add its one-period lag to specify the dynamic SDM.

Table 7. Model Specification Tests for Spatial Econometric Models.

Test	Statistic	Test	Statistic
LM-lag	624.9311 ***	Hausman FE vs. RE	250.9999 ***
LM-error	611.6915 ***	Wald: SDM → SAR	34.4937 ***
Robust LM-lag	26.6467 ***	Wald: SDM → SEM	35.7148 ***
Robust LM-error	13.4071 ***		

Note: The spatial weight matrix is a row-standardized K = 6 nearest-neighbor matrix. *** denotes statistical significance at the 1% level.

Table 8 reports the estimation results from different spatial panel models. In the bias-corrected QML estimates for the dynamic SDM in column (5), the coefficient on L.CUL is 0.6763 and is significant at the 1% level, indicating strong temporal persistence in CUL. The estimated spatial autoregressive coefficient (ρ) is 0.2566 and is significant at the 1% level, indicating positive spatial dependence in CUL after accounting for temporal persistence and other covariates. The estimation results also show that the coefficient of SIA is significantly negative, whereas those of lnPGDP and GOV are significantly positive. Because the coefficients of the SDM do not directly represent marginal effects, this study further decomposes the short- and long-run effects into direct, indirect, and total effects, as reported in Table 9. For the baseline K6 specification, the spectral radius of the estimated

dynamic transition matrix is 0.9097, confirming that the estimated model satisfies the dynamic stability condition required for long-run effect decomposition. The resulting estimates are interpreted as conditional dynamic spatial associations. First, the short- and long-run direct effects of SIA are −0.0289 and −0.1094, respectively, both significant at the 1% level, whereas the corresponding indirect effects are statistically insignificant. This indicates a negative local association between secondary-industry agglomeration and CUL in the baseline model. By contrast, neither the direct nor the indirect effects of TIA are statistically significant, indicating no statistically detectable direct or spatial spillover effects under the current model specification.

Table 8. Estimation Results of Spatial Panel Models.

Variables	(1) TWFE	(2) SAR	(3) SEM	(4) Static SDM	(5) Dynamic SDM
L.CUL	—	—	—	—	0.6763 ***
					(0.0132)
ρ (W·CUL)	—	0.4468 ***	—	0.4487 ***	0.2566 ***
		(0.0207)		(0.0217)	(0.0196)
λ (Spatial error)	—	—	0.4714 ***	—	—
			(0.0213)		
SIA	−0.0529 ***	−0.0627 ***	−0.0672 ***	−0.0692 ***	−0.0281 ***
	(0.0183)	(0.0084)	(0.0090)	(0.0091)	(0.0077)
TIA	0.0397 *	0.0093	0.0182	0.0115	0.0079
	(0.0221)	(0.0104)	(0.0114)	(0.0118)	(0.0099)
lnPGDP	0.0614 ***	0.0462 ***	0.0514 ***	0.0446 ***	0.0180 ***
	(0.0084)	(0.0037)	(0.0041)	(0.0043)	(0.0037)
HC	0.0017	0.0010	0.0008	0.0006	−0.0002
	(0.0014)	(0.0008)	(0.0008)	(0.0008)	(0.0007)
DIG	0.0885	0.0810 ***	0.0855 ***	0.0777 ***	−0.0043
	(0.0639)	(0.0204)	(0.0210)	(0.0212)	(0.0178)
GF	0.0014	−0.0029	−0.0056	−0.0025	−0.0082
	(0.0141)	(0.0090)	(0.0088)	(0.0089)	(0.0075)
GOV	−0.0083	−0.0076	−0.0077	0.0061	0.0289 **
	(0.0296)	(0.0136)	(0.0152)	(0.0157)	(0.0132)
W·SIA	—	—	—	0.0450 ***	−0.0046
				(0.0172)	(0.0145)
W·TIA	—	—	—	0.0107	−0.0331 *
				(0.0210)	(0.0177)
W·lnPGDP	—	—	—	−0.0001	−0.0007
				(0.0070)	(0.0060)
W·HC	—	—	—	0.0020	−0.0017
				(0.0019)	(0.0016)
W·DIG	—	—	—	−0.1102 **	−0.0963 **
				(0.0451)	(0.0379)
W·GF	—	—	—	0.0426 **	0.0194
				(0.0209)	(0.0175)
W·GOV	—	—	—	−0.0208	0.0170
				(0.0260)	(0.0218)
City FE	Yes	Yes	Yes	Yes	Yes
Year FE	Yes	Yes	Yes	Yes	Yes
Adjusted Within R^2	0.0488	—	—	—	—
Pseudo R^2	—	0.9319	0.9204	0.9325	—
Log L	—	8377.960	−1464.986	8395.146	—

Note: The TWFE model reports the adjusted within R^2, while the SAR, SEM, and static SDM report pseudo-R^2 values. Standard errors are shown in parentheses. ***, **, and * denote statistical significance at the 1%, 5%, and 10% levels, respectively.

Table 9. Short- and Long-Run Effect Decomposition of the Dynamic Spatial Durbin Model.

Horizon	Effect Type	SIA	TIA	lnPGDP	HC	DIG	GF	GOV
Short Run	Direct Effect	−0.0289 ***	0.0067	0.0180 ***	−0.0002	−0.0085	−0.0070	0.0295 **
		(0.0074)	(0.0095)	(0.0037)	(0.0006)	(0.0175)	(0.0071)	(0.0124)
	Indirect Effect	−0.0126	−0.0384	0.0043	−0.0022	−0.1308 ***	0.0214	0.0310
		(0.0186)	(0.0243)	(0.0070)	(0.0021)	(0.0482)	(0.0215)	(0.0282)
	Total Effect	−0.0414 **	−0.0317	0.0222 ***	−0.0024	−0.1393 ***	0.0144	0.0605 **
		(0.0199)	(0.0250)	(0.0068)	(0.0022)	(0.0526)	(0.0241)	(0.0267)
Long Run	Direct Effect	−0.1094 ***	0.0029	0.0659 ***	−0.0020	−0.0995	−0.0137	0.1215 ***
		(0.0298)	(0.0361)	(0.0126)	(0.0027)	(0.0743)	(0.0300)	(0.0441)
	Indirect Effect	−0.3930	−0.4011	0.1970 *	−0.0280	−1.5874 *	0.1856	0.6145
		(0.2918)	(0.3558)	(0.1080)	(0.0294)	(0.8271)	(0.2870)	(0.4088)
	Total Effect	−0.5024	−0.3981	0.2629 **	−0.0299	−1.6869 *	0.1718	0.7360 *
		(0.3114)	(0.3770)	(0.1134)	(0.0314)	(0.8792)	(0.3099)	(0.4302)

Note: Indirect effects summarize cross-city associations. Standard errors in parentheses are based on 200 parameter draws from the estimated QML covariance. ***, **, and * denote statistical significance at the 1%, 5%, and 10% levels, respectively.

Economic development shows a positive local association with CUL. The short- and long-run direct estimates for lnPGDP are 0.0180 and 0.0659, respectively, both significant at the 1% level. The short-run indirect estimate is statistically insignificant, while the long-run indirect estimate is positive and significant at the 10% level ($p = 0.0681$). For DIG, the direct estimates are statistically insignificant at both horizons. The short-run indirect estimate is −0.1308 ($p = 0.0067$), and the long-run indirect estimate is −1.5874 ($p = 0.0549$). After removing city and year fixed effects, the correlation between DIG and lnPGDP is −0.085, and the variance inflation factors (VIFs) for DIG and its spatial lag are 1.205 and 1.203, respectively. These diagnostics provide little evidence of substantial multicollinearity involving DIG. The short-run indirect effect indicates a negative spatial association between digital economy development and CUL in neighboring cities. This pattern may reflect differences in digital technology diffusion and the spatial distribution of innovation resources. While digital technologies can facilitate knowledge diffusion and green technology adoption, the concentration of digital industries, skilled labor, and investment in more developed cities may also shape neighboring cities' access to resources for low-carbon transitions. Recent studies provide supporting evidence of heterogeneous spatial environmental effects associated with digital technology innovation and infrastructure development [65,66]. The short- and long-run direct estimates for GOV are 0.0295 and 0.1215, significant at the 5% and 1% levels, respectively. The corresponding indirect estimates are statistically insignificant. Neither HC nor GF exhibits statistically significant direct or indirect associations in the baseline model. The VIFs for HC, GF, and their spatial lags range from 1.009 to 1.080, providing little evidence that substantial multicollinearity accounts for these statistically insignificant estimates. The HC indicator primarily captures the scale of higher education, whereas its relationship with CUL may also depend on workforce skills and the capacity to translate knowledge into green technological applications. For GF, the estimated associations may reflect differences in the allocation of green financial resources and their translation into low-carbon investment. These findings highlight the importance of considering the specific dimensions of human capital and green finance when interpreting their relationships with urban CUL.

4.6. Robustness and Sensitivity Analyses

The robustness and sensitivity analyses address three aspects of the empirical findings: CUL measurement, sample and indicator selection, and spatial model specification. Sensitivity to weighting and aggregation was assessed using equal-weighted linear aggregation, equal-weighted TOPSIS, and coefficient-of-variation weighting with linear aggregation.

The indicator set, directions, and preprocessing remained consistent with the baseline. As reported in Table 10, Pearson correlations with baseline CUL range from 0.9401 to 0.9912, while agreement in the direction of annual mean changes ranges from 92.86% to 100%. These comparisons indicate that the aggregate temporal pattern is broadly consistent across alternative schemes, although individual cities' rankings vary with the weighting and aggregation rules.

Table 10. Sensitivity to Alternative Weighting and Aggregation Schemes.

Alternative Scheme	Pearson Correlation	Spearman Correlation	Agreement in Direction of Annual Mean Change (%)	Mean Absolute Rank Change
Equal-weighted linear aggregation	0.9438	0.9413	92.86%	20.50
Equal-weighted TOPSIS	0.9401	0.9461	92.86%	19.94
Coefficient-of-variation weighting with linear aggregation	0.9912	0.9900	100.00%	8.42

Note: Comparisons use baseline CUL. Agreement refers to the direction of annual mean changes; rank changes are averaged across 4230 city-year observations, with cities ranked within each year.

Indicator-exclusion analyses provide further evidence on measurement sensitivity. Separately excluding foreign trade dependence, the gas penetration rate, and public environmental attention and recalculating the entropy weights produces Pearson correlations of 0.9550, 0.9994, and 0.9761 with baseline CUL, respectively. Joint exclusion of all three indicators yields a correlation of 0.8902, with mean CUL remaining higher in 2024 than in 2010. The corresponding mean absolute change in annual city rankings is approximately 31 positions. Excluding private car ownership yields a correlation of 0.9887 and a mean absolute rank change of 8.36 positions. The reconstructed indices therefore show strong overall correlations with baseline CUL, while the ranking comparisons identify sensitivity to indicator composition.

Sample sensitivity was assessed by excluding cities in the highest decile of original missingness across the CUL indicators, including ties at the cutoff. The resulting sample contains 253 cities. A row-standardized K6 matrix was reconstructed for the retained cities, and the dynamic estimation period remained 2012–2024. Mean CUL remained higher in 2024 than in 2010, annual global Moran's I values remained positive, and the state persistence rate changed from 78.65% to 78.54%. Joint exclusion of the two CUL indicators with the highest missingness rates likewise retained the overall increase in mean CUL and positive spatial clustering.

The exclusion specifications target two concerns: sensitivity to missingness, assessed by excluding high-missingness cities, the two CUL indicators with the highest missingness rates, and HC, the regression covariate with the highest missingness rate; and sensitivity to indicator interpretation, assessed by excluding foreign trade dependence and private car ownership. Table 11 reports the short-run direct and indirect associations of all seven covariates under the sample and indicator exclusions. The positive direct association of lnPGDP and the negative indirect association of DIG are retained, although the latter reaches only the 10% significance level after excluding high-missingness cities. The direct association of SIA remains significantly negative across these specifications. The positive direct association of GOV is less consistent and becomes insignificant following joint exclusion of the two high-missingness indicators. Neither HC nor GF exhibits significant direct or indirect associations in these comparisons. The negative indirect association of TIA reaches the 10% significance level in some specifications, indicating sensitivity to sample and indicator inclusion.

Table 11. Sensitivity to Sample and Indicator Exclusion.

Specification	Effect Type	SIA	TIA	lnPGDP	HC	DIG	GF	GOV
Baseline	Direct	−0.0289 ***	0.0067	0.0180 ***	−0.0002	−0.0085	−0.0070	0.0295 **
	Indirect	−0.0126	−0.0384	0.0043	−0.0022	−0.1308 ***	0.0214	0.0310
Excluding high-missingness cities	Direct	−0.0250 ***	0.0140	0.0204 ***	−0.0004	−0.0086	−0.0077	0.0393 ***
	Indirect	0.0039	−0.0177	0.0023	−0.0016	−0.0907 *	0.0222	0.0474
Excluding two high-missingness indicators	Direct	−0.0376 ***	0.0051	0.0173 ***	−0.0001	−0.0238	0.0009	0.0200
	Indirect	−0.0193	−0.0437 *	0.0000	−0.0025	−0.1218 **	0.0330	0.0144
Excluding HC	Direct	−0.0291 ***	0.0064	0.0179 ***	—	−0.0058	−0.0070	0.0303 **
	Indirect	−0.0159	−0.0396 *	0.0050	—	−0.1180 **	0.0242	0.0270
Excluding foreign trade dependence	Direct	−0.0375 ***	0.0053	0.0254 ***	0.0001	0.0043	−0.0093	0.0226 *
	Indirect	0.0092	−0.0177	−0.0014	−0.0017	−0.1364 **	0.0304	0.0273
Excluding private car ownership	Direct	−0.0303 ***	0.0108	0.0197 ***	−0.0003	−0.0232	−0.0066	0.0327 **
	Indirect	−0.0195	−0.0519 *	0.0034	−0.0022	−0.1445 ***	0.0297	0.0328

Note: Short-run estimates are reported. Inference uses 200 parameter draws from bias-corrected QML models. ***, **, and * indicate significance at 1%, 5%, and 10%, respectively.

Sensitivity to neighborhood definitions was assessed by replacing the baseline K6 matrix with row-standardized K4 and K8 matrices while retaining the sample, covariates, and bias-corrected QML specification. An additional specification introduces one-year lags of all seven covariates and their corresponding spatial lags, with the estimation period remaining 2012–2024. The spatial autoregressive coefficients are positive across specifications, at 0.2566, 0.2241, 0.2761, and 0.2505 for the baseline, K4, K8, and lagged-covariate models, respectively.

As shown in Table 12, the positive short-run direct association of lnPGDP and the negative short-run indirect association of DIG remain significant across these specifications. The direct association of SIA remains significantly negative under K4 and K8 but becomes insignificant when covariates are lagged. GOV retains a positive direct association, whereas its indirect association reaches the 10% significance level only under K8. A positive indirect association of GF is significant at the 10% level only in the lagged-covariate model. These results distinguish relatively consistent short-run patterns from associations that depend more strongly on model specification. The long-run indirect association of DIG is more sensitive to neighborhood definitions, with p-values of 0.0549, 0.0232, and 0.2478 under K6, K4, and K8, respectively. Interpretation consequently places greater emphasis on its short-run cross-city association, which receives more consistent statistical support.

Table 12. Sensitivity to Spatial Weights and Lagged Covariates.

Specification	Effect Type	SIA	TIA	lnPGDP	HC	DIG	GF	GOV
Baseline (K6)	Direct	−0.0289 ***	0.0067	0.0180 ***	−0.0002	−0.0085	−0.0070	0.0295 **
	Indirect	−0.0126	−0.0384	0.0043	−0.0022	−0.1308 ***	0.0214	0.0310
Alternative weights (K4)	Direct	−0.0284 ***	0.0082	0.0183 ***	0.0000	−0.0074	−0.0070	0.0278 **
	Indirect	−0.0032	−0.0271	0.0027	−0.0021	−0.1003 ***	0.0209	0.0311
Alternative weights (K8)	Direct	−0.0289 ***	0.0065	0.0177 ***	−0.0004	−0.0105	−0.0069	0.0289 **
	Indirect	0.0089	−0.0215	0.0022	−0.0021	−0.1690 ***	0.0188	0.0608 *
Lagged covariates (K6)	Direct	0.0009	0.0028	0.0124 ***	−0.0012	−0.0215	−0.0059	0.0278 **
	Indirect	0.0145	0.0065	−0.0043	−0.0023	−0.1311 ***	0.0478 *	0.0349

Note: All associations are short-run estimates. Inference uses 200 parameter draws from bias-corrected QML models. ***, **, and * indicate significance at 1%, 5%, and 10%, respectively.

Alternative measures of DIG and GF were also examined. Within a matched sample of 275 cities using the same years and spatial matrix, the original DIG composite index retains a negative short-run indirect association (-0.1031, $p = 0.0429$), whereas the corresponding estimate for broadband penetration is insignificant ($p = 0.8447$). This difference indicates that the estimated association depends partly on the dimension of digital development measured. With an equal-weighted GF index, the short-run direct and indirect associations remain insignificant ($p = 0.3210$ and 0.4240, respectively). The negative short-run cross-city

association remains significant when DIG is measured by the original composite index in the matched sample, while the GF results remain consistent under equal weighting.

5. Conclusions and Policy Implications

5.1. Conclusions

Using panel data for 282 Chinese cities at or above the prefecture level from 2010 to 2024, this study constructs a composite CUL index and systematically examines its evolution and associated factors from three perspectives: dynamic evolution, state transitions, and spatial spillovers. The main conclusions are as follows. First, CUL levels exhibit a generally upward trend, with variations in the pace of improvement over time. From 2010 to 2016, CUL increased steadily; after 2017, it entered a period of more rapid growth and remained at relatively high levels during 2019–2021. Although some adjustment occurred thereafter, the overall level remained substantially higher than at the beginning of the study period. Meanwhile, intercity disparities did not narrow consistently with the overall improvement in CUL, and high-level cities continued to maintain relative advantages, indicating persistent differences in CUL levels across cities. Second, CUL exhibits significant positive spatial dependence and clustering among cities with similar levels. Global Moran's I remained significantly positive throughout the sample period, with H-H and L-L clustering constituting the dominant spatial patterns. Relatively stable high-value clusters emerged among some cities in the Yangtze River Delta and Pearl River Delta, whereas some resource-based and traditional industrial cities persistently exhibited low-value clustering. Although the overall degree of spatial autocorrelation declined after 2018, low-value clustering remained highly persistent, indicating a certain degree of stability in the spatial pattern of CUL. Third, CUL state transitions exhibit strong persistence, gradualism, and neighborhood dependence. Persistence probabilities are generally high across states, particularly for the low and high states, while transitions occur predominantly between adjacent states and nonadjacent-state transitions remain rare. The spatial Markov results further show that state transition probabilities vary considerably across different neighborhood conditions. Higher-state neighborhoods are associated with greater probabilities of upward transitions among cities in low and intermediate states, and the probability of moving from State III to State IV increases as the neighborhood state rises, indicating pronounced neighborhood-condition dependence in the evolution of CUL states. Fourth, CUL exhibits significant temporal persistence and positive spatial dependence. Economic development shows positive short- and long-run local associations, while its short-run indirect association is statistically insignificant. The digital economy exhibits a negative short-run cross-city association that remains significant across alternative nearest-neighbor matrices and lagged-covariate specifications; its long-run association is more sensitive to model specification. Secondary-industry agglomeration shows a negative local association in the baseline model, but this association becomes insignificant when covariates are lagged. Government intervention exhibits a positive local association, although its significance is sensitive to indicator exclusion. Tertiary-industry agglomeration, human capital, and green finance show no statistically significant direct or indirect associations in the baseline model. These findings are interpreted as conditional dynamic spatial associations.

5.2. Policy Implications

Based on the above findings, this study proposes the following policy implications, with particular attention to state persistence, neighborhood dependence, and differences in the associations of relevant factors with CUL. First, long-term transition policies should be tailored to the strong persistence of low CUL states. The spatial Markov results show that both low and high states exhibit substantial persistence, with the persistence probability

of the low state reaching 81.62% and transitions between non-adjacent states remaining rare. This suggests that CUL evolves gradually and that short-term emission-reduction measures alone are unlikely to fundamentally alter long-standing lock-in conditions. For cities with strong resource dependence and traditional industrial bases, policy priorities should therefore shift from short-term emission control toward industrial restructuring, the upgrading of high-carbon assets, and the substitution of low-carbon technologies, thereby continuously improving the internal conditions required for upward transitions in CUL states. Second, neighborhood conditions should be better leveraged to improve the external environment for CUL. The spatial Markov results indicate substantial differences in transition probabilities across neighborhood states. In particular, the probability of moving from State III to State IV rises markedly as the neighborhood state improves, whereas lower-state neighborhoods are associated with stronger constraints on upward transitions. Policies should therefore facilitate the orderly diffusion of green technologies, low-carbon industries, and public governance experience across cities, strengthen technological, industrial, and factor linkages between lower- and higher-state cities, and improve the external conditions that enable cities in low and intermediate states to move upward. At the same time, regions characterized by persistent L-L clustering should seek to prevent the long-term spatial entrenchment of low CUL states. Third, policy priorities should reflect the different associations of industrial agglomeration, economic development, and government intervention with CUL. The negative local association of secondary-industry agglomeration in the baseline model supports attention to technological upgrading, cleaner energy use, and structural optimization in traditional industrial cities. Its sensitivity to covariate timing also highlights the need to consider local industrial conditions when designing interventions. Economic development exhibits positive local associations over both short and long horizons, suggesting that growth strategies could be coordinated with low-carbon investment and industrial upgrading. The positive local association of government intervention provides further motivation to assess the allocation and effectiveness of fiscal support for green technologies, energy-efficiency retrofits, and low-carbon infrastructure. Fourth, digital development policies should give greater consideration to cross-city coordination. The negative short-run indirect association of DIG remains significant across alternative nearest-neighbor matrices and lagged-covariate specifications, indicating the value of assessing neighboring cities' transition conditions alongside local digital development. Digital infrastructure investment and transformation programs could therefore incorporate cross-regional connectivity, technology-service sharing, and digital capacity building in surrounding cities. Monitoring the distribution of low-carbon benefits across participating cities would help evaluate whether such coordination supports more balanced transition outcomes.

Author Contributions: Z.Y.; data curation, N.W.; writing—original draft preparation, Z.Y.; writing—review and editing, Z.Z.; supervision, Z.Z.; project administration, Z.Z. All authors have read and agreed to the published version of the manuscript.

Funding: This research was funded by the Major Program of the National Social Science Fund of China (grant number 22&ZD109).

Institutional Review Board Statement: Not applicable.

Informed Consent Statement: Not applicable.

Data Availability Statement: The data supporting the findings of this study are available from the corresponding author upon reasonable request, subject to applicable third-party data access restrictions.

Conflicts of Interest: The authors declare no conflicts of interest. The funders had no role in the design of the study; in the collection, analyses, or interpretation of data; in the writing of the manuscript; or in the decision to publish the results.

References

1. Unruh, G.C. Understanding carbon lock-in. *Energy Policy* **2000**, *28*, 817–830. [CrossRef]
2. Seto, K.C.; Davis, S.J.; Mitchell, R.B.; Stokes, E.C.; Unruh, G.; Ürge-Vorsatz, D. Carbon lock-in: Types, causes, and policy implications. *Annu. Rev. Environ. Resour.* **2016**, *41*, 425–452. [CrossRef]
3. Zhu, Y.; Rao, H. Does low carbon city pilot promote urban carbon unlocking?—A heterogeneity analysis based on machine learning. *Cities* **2024**, *147*, 104815. [CrossRef]
4. Mao, W.; Wang, W.; Sun, H.; Yao, P.; Wang, X.; Luo, D. Urban industrial transformation patterns under natural resource dependence: A rule mining technique. *Energy Policy* **2021**, *156*, 112383. [CrossRef]
5. Xie, L.; Hui, S. Low-carbon transition policy and employment structure: Evidence from China's Low-carbon City Pilot. *Cities* **2025**, *162*, 105985. [CrossRef]
6. Zhao, C.; Dong, K.; Wang, K.; Taghizadeh-Hesary, F. How can Chinese cities escape from carbon lock-in? The role of low-carbon city policy. *Urban Clim.* **2023**, *51*, 101629. [CrossRef]
7. Peng, X. Strategic interaction of environmental regulation and green productivity growth in China: Green innovation or pollution refuge? *Sci. Total Environ.* **2020**, *732*, 139200. [CrossRef]
8. Tang, Z.; Yu, H.; Zou, J. Neighbor impacts of environmental regulation: The case of low-carbon pilot program in China. *Energy* **2023**, *276*, 127509. [CrossRef]
9. Shi, Y.; Zhao, Y. Evolutionary characteristics and driving mechanisms of the spatial association network of carbon unlocking in the Yangtze River Delta urban agglomeration. *Sci. Rep.* **2026**, *16*, 31843. [CrossRef]
10. Arthur, W.B. Competing technologies, increasing returns, and lock-in by historical events. *Econ. J.* **1989**, *99*, 116–131. [CrossRef]
11. Cowan, R.; Hultén, S. Escaping lock-in: The case of the electric vehicle. *Technol. Forecast. Soc. Change* **1996**, *53*, 61–79. [CrossRef]
12. Unruh, G.C. Escaping carbon lock-in. *Energy Policy* **2002**, *30*, 317–325. [CrossRef]
13. Liu, S.; Guo, Y.; Wagner, F.; Liu, H.; Cui, R.Y.; Mauzerall, D.L. Diversifying heat sources in China's urban district heating systems will reduce risk of carbon lock-in. *Nat. Energy* **2024**, *9*, 1021–1031. [CrossRef]
14. Schuch, E.; Apergi, M.; Chow, D.Y.K.; Eicke, L.; Goldthau, A.; Kurniawan, J.H.; Lima-de-Oliveira, R.; Tan, Z.G.; Weko, S. Breaking the carbon lock-in: Identifying pathways for Malaysia towards a low-carbon future. *Technol. Forecast. Soc. Change* **2024**, *202*, 123331. [CrossRef]
15. Erickson, P.; Kartha, S.; Lazarus, M.; Tempest, K. Assessing carbon lock-in. *Environ. Res. Lett.* **2015**, *10*, 084023. [CrossRef]
16. Niu, H.; Liu, Z. Measurement on carbon lock-in of China based on RAGA-PP model. *Carbon Manag.* **2021**, *12*, 451–463. [CrossRef]
17. Wang, S.; Shi, C.; Fang, C.; Feng, K. Examining the spatial variations of determinants of energy-related CO_2 emissions in China at the city level using Geographically Weighted Regression Model. *Appl. Energy* **2019**, *235*, 95–105. [CrossRef]
18. Zhao, C.; Ma, X.; Che, S.; Liu, Z.; Song, C. Does climate aid alleviate carbon lock-in? A global perspective. *J. Clean. Prod.* **2024**, *449*, 141782. [CrossRef]
19. Zhou, C.; Qi, S. Can carbon emission trading policy break China's urban carbon lock-in? *J. Environ. Manag.* **2024**, *353*, 120129. [CrossRef]
20. Cantoni, R.; Brisbois, M.C. En route to decarbonization: A periodisation of just transition in four carbon-intensive EU regions. *Geoforum* **2024**, *154*, 104061. [CrossRef]
21. Bourdin, S.; Perrot, A. Breaking free from the regional carbon trap: Analysing the persistence of CO_2 emissions in EU regions. *Camb. J. Reg. Econ. Soc.* **2026**, *19*, 49–67. [CrossRef]
22. Geels, F.W. Escaping and creating lock-ins in accelerating low-carbon transitions: Conceptual reflections and empirical insights from electricity and auto-mobility transitions in Europe, the USA and China. *Camb. J. Reg. Econ. Soc.* **2026**, *19*, 251–273. [CrossRef]
23. Xu, W.; Mo, W. Institutional unlocking or technological unlocking? The logic of carbon unlocking in the new energy vehicle industry in China. *Energy Policy* **2024**, *195*, 114369. [CrossRef]
24. Ruan, W.; Zhang, H.; Yang, J. How to break carbon lock-in of thermal power industry in China—A tripartite evolutionary game analysis. *Appl. Energy* **2025**, *377*, 124504. [CrossRef]
25. Hu, Z.; Xu, Y. Can new energy demonstration cities break through the multiple carbon lock-in? Evidence based on double machine learning. *Energy Policy* **2025**, *199*, 114522. [CrossRef]
26. Shen, N.; Zhang, L.; Wang, Q.; Wu, L. The power of institutional innovation in the urban carbon unlocking: A study on collaborative empowerment of digital policy and new energy policy. *Energy Policy* **2025**, *206*, 114721. [CrossRef]
27. Wen, J.; Zhou, Y. Trade openness and urban green innovation: A dual perspective based on financial agglomeration and human capital accumulation. *Sustain. Futur.* **2025**, *9*, 100478. [CrossRef]
28. Davis, S.J.; Caldeira, K.; Matthews, H.D. Future CO_2 emissions and climate change from existing energy infrastructure. *Science* **2010**, *329*, 1330–1333. [CrossRef]
29. Pfeiffer, A.; Millar, R.; Hepburn, C.; Beinhocker, E. The '2 °C capital stock' for electricity generation: Committed cumulative carbon emissions from the electricity generation sector and the transition to a green economy. *Appl. Energy* **2016**, *179*, 1395–1408. [CrossRef]

30. Song, C.; Guo, Z.; Ma, X.; He, J.; Liu, Z. Evaluating the role of next-generation productive forces in mitigating carbon lock-in: Evidence from regional disparities in China. *Sustainability* **2025**, *17*, 4241. [CrossRef]
31. Wang, C.; Wang, W.; Zhou, J. Does the new energy vehicles policy promote urban carbon unlocking? The case of China. *Int. Rev. Econ. Financ.* **2026**, *111*, 105641. [CrossRef]
32. Weng, S.; Song, M.; Tao, W.; Chen, J.; Chen, H. Breaking the inertia of urban energy systems: Does the new energy demonstration city construction improve carbon unlocking efficiency? *Renew. Energy* **2025**, *244*, 122672. [CrossRef]
33. Zhao, F.; Hu, Z.; Zhao, X. Does innovative city construction improve urban carbon unlocking efficiency? Evidence from China. *Sustain. Cities Soc.* **2023**, *92*, 104494. [CrossRef]
34. Weng, S.; Benkraiem, R.; Nghiem, X.-H.; Zhao, X.; Xu, J. Market tools for achieving carbon unlocking: Is China's energy-consumption trading policy effective? *J. Environ. Manag.* **2025**, *389*, 126162. [CrossRef]
35. Xing, P.; Wang, Y.; Ye, T.; Sun, Y.; Li, Q.; Li, X.; Li, M.; Chen, W. Carbon emission efficiency of 284 cities in China based on machine learning approach: Driving factors and regional heterogeneity. *Energy Econ.* **2024**, *129*, 107222. [CrossRef]
36. Cheng, H.; Wu, B.; Jiang, X. Study on the spatial network structure of energy carbon emission efficiency and its driving factors in Chinese cities. *Appl. Energy* **2024**, *371*, 123689. [CrossRef]
37. Wei, M.; Cai, Z.; Song, Y.; Xu, J. Spatiotemporal evolutionary characteristics and driving forces of carbon emissions in three Chinese urban agglomerations. *Sustain. Cities Soc.* **2024**, *104*, 105320. [CrossRef]
38. Wang, Z.; Shao, H. Spatiotemporal interactions and influencing factors for carbon emission efficiency of cities in the Yangtze River Economic Belt, China. *Sustain. Cities Soc.* **2024**, *103*, 105248. [CrossRef]
39. Gao, J.; Zhao, S.; Wang, L.; Wang, X. Spatiotemporal analysis of carbon emissions in the Yangtze River Delta Urban Agglomeration: Insights from nighttime light data (1992–2019). *Ecol. Inform.* **2024**, *83*, 102831. [CrossRef]
40. Wu, H.; Yang, Y.; Li, W. Dynamic spatiotemporal evolution and spatial effect of carbon emissions in urban agglomerations based on nighttime light data. *Sustain. Cities Soc.* **2024**, *113*, 105712. [CrossRef]
41. Wu, C.; Deng, H.; Zhao, H.; Xia, Q. Spatiotemporal evolution and convergence patterns of urban carbon emission efficiency in China. *Humanit. Soc. Sci. Commun.* **2025**, *12*, 675. [CrossRef]
42. Liu, Y.; Wu, Y.; Zhang, M. Specialized, diversified agglomeration and CO_2 emissions—An empirical study based on panel data of Chinese cities. *J. Clean. Prod.* **2024**, *467*, 142892. [CrossRef]
43. Du, C.; Cao, Y.; Ling, Y.; Jin, Z.; Wang, S.; Wang, D. Does manufacturing agglomeration promote green productivity growth in China? Fresh evidence from partially linear functional-coefficient models. *Energy Econ.* **2024**, *131*, 107352. [CrossRef]
44. Barbero, J.; Diukanova, O.; Gianelle, C.; Salotti, S.; Santoalha, A. Technologically related diversification: One size does not fit all European regions. *Res. Policy* **2024**, *53*, 104973. [CrossRef]
45. Vrontisi, Z.; Charalampidis, I.; Fragkiadakis, K.; Florou, A. Towards a just transition: Identifying EU regions at a socioeconomic risk of the low-carbon transition. *Energy Clim. Change* **2024**, *5*, 100129. [CrossRef]
46. Almazán-Gómez, M.Á.; Llano, C.; Pérez, J. Putting off the coal in Europe: Socio-economic trade-offs across the European regions. *Energy Policy* **2024**, *195*, 114360. [CrossRef]
47. Xu, Y.; Dong, B.; Chen, Y.; Qin, H. Effect of industrial transfer on carbon lock-in: A spatial econometric analysis of Chinese cities. *J. Environ. Plan. Manag.* **2022**, *65*, 1024–1055. [CrossRef]
48. Corrocher, N.; Grabner, S.M.; Morrison, A. Green technological diversification: The role of international linkages in leaders, followers and catching-up countries. *Res. Policy* **2024**, *53*, 104972. [CrossRef]
49. Lee, C.-C.; Wang, T. The impact of renewable energy policies on the energy transition—An empirical analysis of Chinese cities. *Energy Econ.* **2024**, *138*, 107838. [CrossRef]
50. Glennon, B. Skilled immigrants, firms, and the global geography of innovation. *J. Econ. Perspect.* **2024**, *38*, 3–26. [CrossRef]
51. Cheng, Y.; Zhang, Y.; Wang, J.; Jiang, J. The impact of the urban digital economy on China's carbon intensity: Spatial spillover and mediating effect. *Resour. Conserv. Recycl.* **2023**, *189*, 106762. [CrossRef]
52. Yang, S.; Li, H.; Liu, X.; Wei, Y.; Shen, J.; Cheng, B. Spatial analysis of the digital economy's influence on urban sustainable development: A decade-long study of Chinese prefecture-level cities. *Ecol. Indic.* **2024**, *166*, 112338. [CrossRef]
53. Wang, L.; Cao, Y.; Hu, J.; Skibniewski, M.J. Does digital economy development benefit low-carbon transition: Evidence based on urban carbon lock-in. *J. Environ. Plan. Manag.* **2026**, *69*, 599–627. [CrossRef]
54. Cifuentes-Faura, J.; Khan, K.; Khurshid, A. Does digital financial inclusion support carbon neutrality? A cross-regional study. *Financ. Innov.* **2026**, *12*, 36. [CrossRef]
55. Liu, Y.; Zhao, C.; Dong, K.; Wang, K.; Sun, L. How does green finance achieve urban carbon unlocking? Evidence from China. *Urban Clim.* **2023**, *52*, 101742. [CrossRef]
56. Zhang, W.; Liu, X.; Zhao, S.; Tang, T. Does green finance agglomeration improve carbon emission performance in China? A perspective of spatial spillover. *Appl. Energy* **2024**, *358*, 122561. [CrossRef]
57. Cifuentes-Faura, J.; Alofaysan, H.; Radulescu, M.; Doğan, B. Dynamic spillover effect among carbon finance, bitcoin, and green energy markets: A novel decomposed connectedness and portfolio analysis. *Financ. Innov.* **2026**, *12*, 109. [CrossRef]

58. Xu, Y.; Xu, F.; Chi, G.; Gong, Z. Carbon emissions and government interventions in urban agglomerations of China: An integrated GWR and neural network approach. *Appl. Geogr.* **2025**, *179*, 103645. [CrossRef]
59. Hermwille, L.; Brisbois, M.C.; Hiteva, R.; Yazar, M.; Nacke, L.; Jewell, J.; Sovacool, B.K.; Cantoni, R.; Oei, P.-Y.; Walk, P.; et al. Compounding injustices can impede a just energy transition. *Nat. Energy* **2025**, *10*, 915–918. [CrossRef]
60. Shannon, C.E. A mathematical theory of communication. *Bell Syst. Tech. J.* **1948**, *27*, 379–423. [CrossRef]
61. Yu, J.; de Jong, R.; Lee, L.F. Quasi-maximum likelihood estimators for spatial dynamic panel data with fixed effects when both n and T are large. *J. Econom.* **2008**, *146*, 118–134. [CrossRef]
62. Lee, L.F.; Yu, J. A spatial dynamic panel data model with both time and individual fixed effects. *Econom. Theory* **2010**, *26*, 564–597. [CrossRef]
63. Ou, Y.; Chen, K.; Ma, L.; He, B.-J.; Bao, Z. Coordinating public and government responses to air pollution exposure: A multi-source data fusion approach. *J. Environ. Manag.* **2024**, *370*, 123024. [CrossRef]
64. Zheng, X.; Zhang, L.; Bai, Y.; Cong, J.; Zhang, T.; Ren, Y.; Li, J.; Su, Y.; Xu, J.; Wang, C. Heterogeneous household responses and indoor temperature inequality in the clean heating transition. *Engineering* **2026**, *65*, 163–171. [CrossRef]
65. Li, S.; Zhang, Z.; Lee, C.-C. The spillover effects of digital technology innovation on carbon emissions in urban agglomerations: A perspective based on manufacturing investment networks and geospatial spillovers. *Sustain. Cities Soc.* **2025**, *124*, 106321. [CrossRef]
66. Zhang, H.; Zhang, K.; Yan, T.; Cao, X. The impact of digital infrastructure on regional green innovation efficiency through industrial agglomeration and diversification. *Humanit. Soc. Sci. Commun.* **2025**, *12*, 220. [CrossRef]

Disclaimer/Publisher's Note: The statements, opinions and data contained in all publications are solely those of the individual author(s) and contributor(s) and not of MDPI and/or the editor(s). MDPI and/or the editor(s) disclaim responsibility for any injury to people or property resulting from any ideas, methods, instructions or products referred to in the content.